

63.3-2

BBE63-002  
Space Science Laboratory

CATALOGED BY ASTIA  
AS AD No. 403 392

HIGH TEMPERATURE EMISSIVITIES  
OF THE 2.7 MICRON BAND OF  $H_2O$   
BETWEEN 1000°K AND 2200°K

CARMINE C. FERRISO  
AND  
CLAUS B. LUDWIG

APRIL 1963

TECHNICAL REPORT  
ENGINEERING DEPARTMENT



GIIIIIID

GENERAL DYNAMICS | ASTRONAUTICS

BBE63-002  
Space Science Laboratory

HIGH TEMPERATURE EMISSIVITIES  
OF THE 2.7 MICRON BAND OF  $H_2O$   
BETWEEN 1000°K AND 2200°K

Carmine C. Ferriso  
and  
Claus B. Ludwig

April 1963

Technical Report

This work was supported by Project DEFENDER,  
Advanced Research Projects Agency, AO 237,  
through the Office of Naval Research, Nonr-3902(00).

**GIIIIID**  
**GENERAL DYNAMICS | ASTRONAUTICS**

High Temperature Emissivities of  
the 2.7 Micron Band of  $H_2O$   
Between 1000°K and 2200°K

By  
C. C. Ferriso and C. B. Ludwig  
Space Science Laboratory  
General Dynamics/Astronautics  
San Diego, California

ABSTRACT

Spectral emissivities between  $2800\text{ cm}^{-1}$  and  $4200\text{ cm}^{-1}$  have been obtained for water vapor at 1000°, 1200°, 1500°, 1800° and 2200°K. The heated  $H_2O$  test gas was produced at the exit of a small rocket burner which used  $H_2$  and  $O_2$  propellants. The emission measurements of the gases were made at the immediated exit of the burner where the composition, total pressures and temperature can be defined. The emissivities or absorptivities were calculated from a calibrated emission spectrum and an accurate spectroscopic determination of the temperature of the test gas. The composition of  $H_2O$  was evaluated from a semi-empirical fit to a thermo-chemical flow calculation.

The hot  $H_2O$  samples were observed at a total pressure of one atmosphere in the optically thin region where the spectral emissivities are on the average approximately 0.05. The variation of the spectral emissivities of  $H_2O$  in the 2.7 micron region as a function of temperature are given for a constant amount of  $H_2O$  in the optical path. A good estimate of the integrated intensity of the 2.7 micron  $H_2O$  band ( $\nu_1$  and  $\nu_3$ ) has been made from the high temperature data.

## INTRODUCTION

The determination of basic spectra absorption or emission parameter of  $H_2O$  at elevated temperatures is of importance for obtaining the radiant infrared power emitted from the exhaust of rocket motors. The quantitative infrared absorption 2.7 micron  $H_2O$  band has been extensively studied at room temperature<sup>1</sup> although an accurate determination of the integrated intensities of this band has not been made. Measurements of the absorption of this band under various pressure, and optical lengths have been made up to approximately  $1500^\circ K$ <sup>2,3</sup> using a cell in a furnace. These measurements were generally made in the optically thick region because of the great problems associated with measuring very small absorptions. These results give information regarding pressure broadening effects and ratios of line widths to line spacings. It is also necessary to measure the spectral absorption of the 2.7 micron  $H_2O$  band at elevated temperatures in the optically thin region where the absorption is small in order to evaluate the average absorption coefficients and perhaps the integrated intensity of the band.

In general, all of the aforementioned basic information are necessary in order to properly evaluate theoretical band models which can be used to predict the quantitative infrared behavior of various hot gas systems.

The present report describes emissivity measurements in the 2.7 micron  $H_2O$  band at one atmosphere total pressure between  $1000^\circ K$  and  $2200^\circ K$ . The hot  $H_2O$  gas samples were the exit gases of a small research rocket burner. The temperature variation of the gases is obtained varying the stoichiometry of the gases,  $H_2$  and  $O_2$ , burned in the rocket. Then present experiments were performed on the gases at the immediate exit of the burner nozzle where the hot exhaust can be well characterized by measuring a radiation gas temperature and using a thermochemical flow calculation to determine the composition of hot  $H_2O$  in the test sample. The other species present in the exhaust are  $O_2$  and a small amount of  $OH$ . Unlike the previous absorption measurements the present results were obtained from calibrated emission spectra and an experimental determination of temperature. These two experimental measurements yield the spectral emissivity or the transmission. As opposed to other absorption measurements in furnaces, the present emission burner technique has its own particular merits and limitations.

## EXPERIMENTAL

Spectrometer System - Fig. 1 shows an overall run of the experimental apparatus which was used to determine the emission spectrum of  $\text{H}_2\text{O}$  in the hot burner gases. The emission measurements were made with a double-pass prism ( $\text{CaF}_2$ ) monochromator, Perkin-Elmer 99, together with a globar light source, thermocouple detector, and a standard blackbody calibration source. The system has been used previously for the hot  $\text{CO}_2$  absorption measurements in the  $4.3\mu$  region and has been described in detail<sup>4</sup>. A wavenumber calibration of the monochromator was made in the usual way using known absorption band of various gases. A wavenumber calibration check was made during each run. For the calibrated emission and temperature measurements, the two position diagonal mirror can be rotated to fill the identical monochromator aperture with a standard blackbody for an energy calibration. For absorption determinations a diminution in the globar intensity was measured. The mechanical slit widths used in the present work was 100 microns, resulting in a spectral slit width of  $5\text{ cm}^{-1}$  at  $2800\text{ cm}^{-1}$  and  $17\text{ cm}^{-1}$  at  $4400\text{ cm}^{-1}$ .

A large insulating box is placed over the apparatus to protect it from the hot rocket exhaust and serves as a convenient enclosure for flushing. The interfering absorption of atmospheric water vapor in the optical path was reduced to less than 10% at the peak absorption by flushing the box containing the optical system with dry nitrogen. An additional percentage of absorption is present from the air in the space between the outer boundary of the exhaust jet and the entrance of the box because of the pumping action of the burner. Since the distance is about 1 cm and the total optical path in the box approximately 3 m, this amounts to about 3%. The opening of the protective box is not protected by a window and the possibility exists that in spite of the flushing procedure, atmospheric air is pushed in during the firing of the rocket; however, no change of absorption is observed in attempting to observe this effect. On the other hand, the globar emission was influenced during runs from turbulent air entering the protective box containing the globar. A  $\text{CaF}_2$  window in front of the globar eliminated this problem. The window was installed at an angle to avoid reflection from the rocket plume.

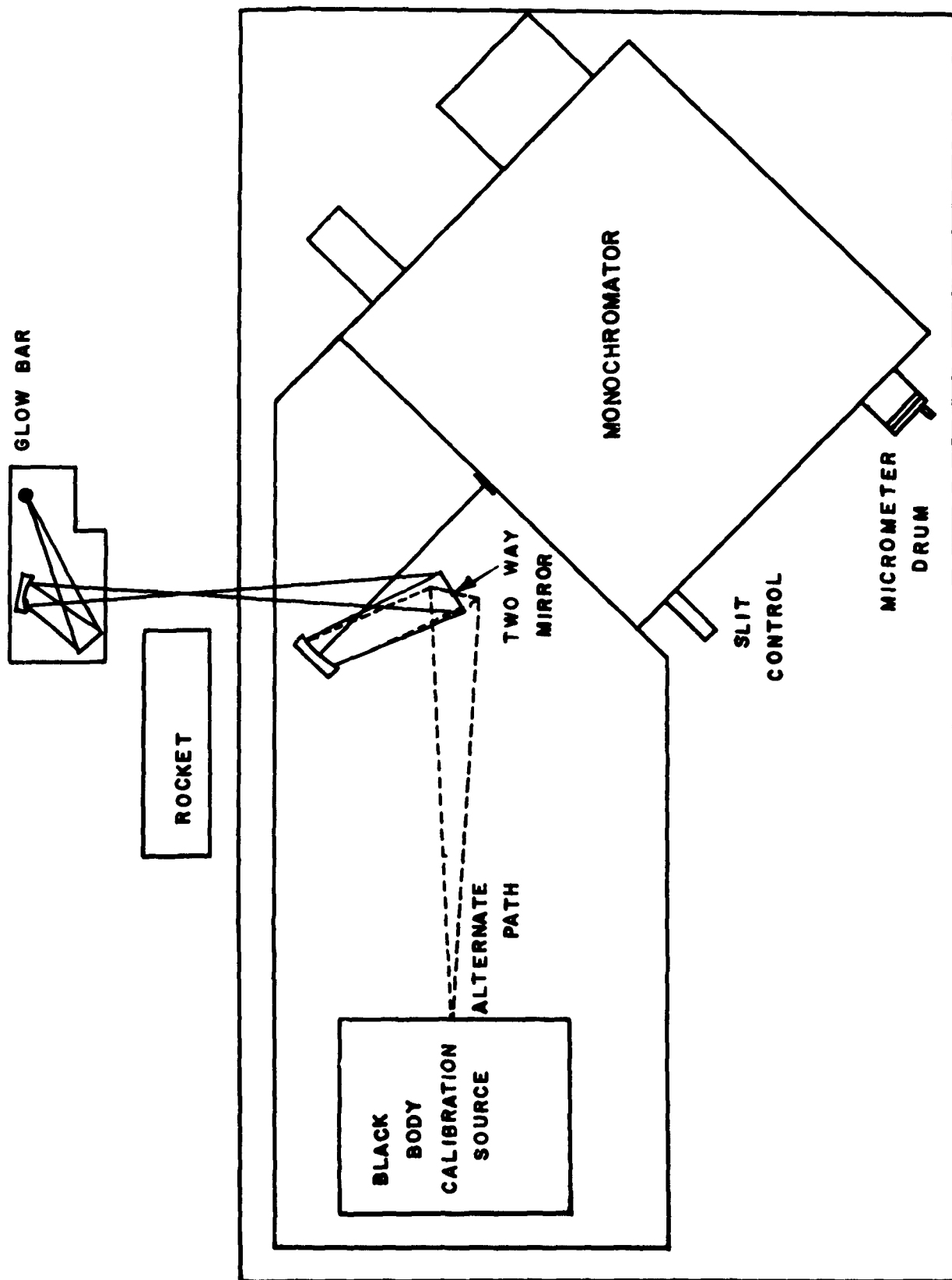


FIGURE 1: SCHEMATIC OF EXPERIMENTAL APPARATUS

Rocket Burner - The supersonic burner which was used to produce the hot gas sample was designed and operates to produce a homogeneous axial jet of characterized gases. A schematic of the burner is shown in Fig. 2. The detail design, performance, and some preliminary results have been reported previously<sup>5</sup>. However, since a combination of hydrogen (instead of kerosene) as fuel and oxygen is being used, the injector part has been modified to insure efficient rocket operation for stoichiometric as well as very lean mixture ratios. The other parts of the burner, namely the chamber nozzle (with an area ratio of 5.25:1) and the water cooling system were not changed. Only the gas supply (gaseous hydrogen and oxygen) was newly installed and the metering system for measuring mass flow was improved. The mass flow ratio is monitored by calibrated orifices and accurate  $\Delta p$ -gauges. The chamber pressure line is connected to the injector face. Attempts to measure the pressure variation in the chamber by placing a second meter near the throat had to be abandoned since hot spots developed where the tube was imbedded into the chamber walls. The exit pressure was measured directly at the end of the nozzle. All the burner operating parameters are made within  $\pm 2\%$ .

Two different injector designs have been employed, which operate under (a), single impingement of fuel and oxidizer and (b), double impingement of fuel and oxidizer. The design (a) is simple to manufacture but is limited to a small range of operation, because the injector holes and angles of impingement are dependent upon the mixture ratios. The design (b) is more complex but permits its use with a wide range of mixing ratios as well as with different fuels. The latter fact is important in view of the continuing program in which a combination of hydrogen, carbon-monoxide and oxygen is used. The design principles of (b) will be presented in a separate report<sup>6</sup>.

The diameter of the exhaust jet (i.e., the geometrical pathlength) was 3.12 cm and the exit gas pressure was always adjusted to one atmosphere. The long term stability in operation was excellent. The performance of the engine was judged by comparing the experimental and theoretical characteristic velocity  $C^*$ . As a first step, the actual chamber pressures versus mixture ratios ( $O_2/H_2$  by weight) were determined. The characteristic velocities were determined by:

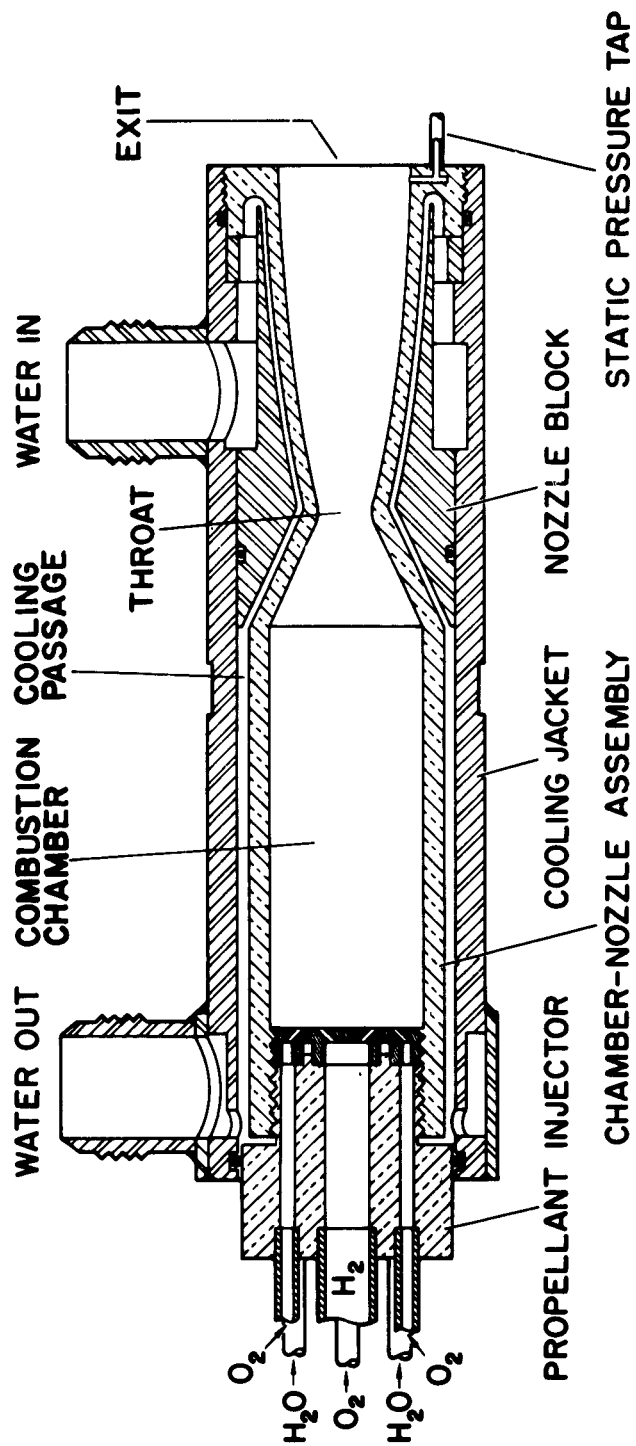


FIGURE 2: SCHEMATIC OF ROCKET BURNER-EXIT DIAMETER 3.12 cm



$$C_{exp}^* = \frac{P_c A_t g}{\dot{w}} \text{ ft/sec}$$

and

$$C_{theor}^* = \left\{ \frac{RT_c}{\bar{k} \bar{Mw}} g \left( \frac{k+1}{2} \right)^{\frac{k+1}{k-1}} \right\}^{1/2} \text{ ft/sec}$$

where

- $P_c$  = chamber pressure, psi
- $A_t$  = throat area, 0.226 in<sup>2</sup>
- $g$  = 32.2 ft/sec<sup>2</sup>
- $\dot{w}$  = total (fuel and oxidizer) mass flow, lbs/sec
- $T_c$  = chamber temperature, °R
- $\bar{Mw}$  = average molecular weight, lbs/Mole
- $\bar{k}$  = average specific heat ratio between chamber and throat
- $k$  = average specific heat ratio at the throat
- $R$  = 1544 ft-lbs/Mole °R

The average molecular weight, the specific heat ratio at the exit and chamber temperatures have been calculated by means of the Astronautics computer program, "Performance Evaluation of Engines and Propellants (PEEP)"<sup>7</sup>. The variation of the specific heat between chamber, throat and exit is very small (±2%) and the exit  $k$  has been used. A comparison of experimental and calculated  $C^*$  is shown in Fig. 3. The difference between frozen and shifting equilibrium is very small because of the small change in  $k$  and molecular weight (see Fig. 3). In comparing the experimental and theoretical  $C^*$  it is found that the engine is operating at an efficiency of better than 95%. Only

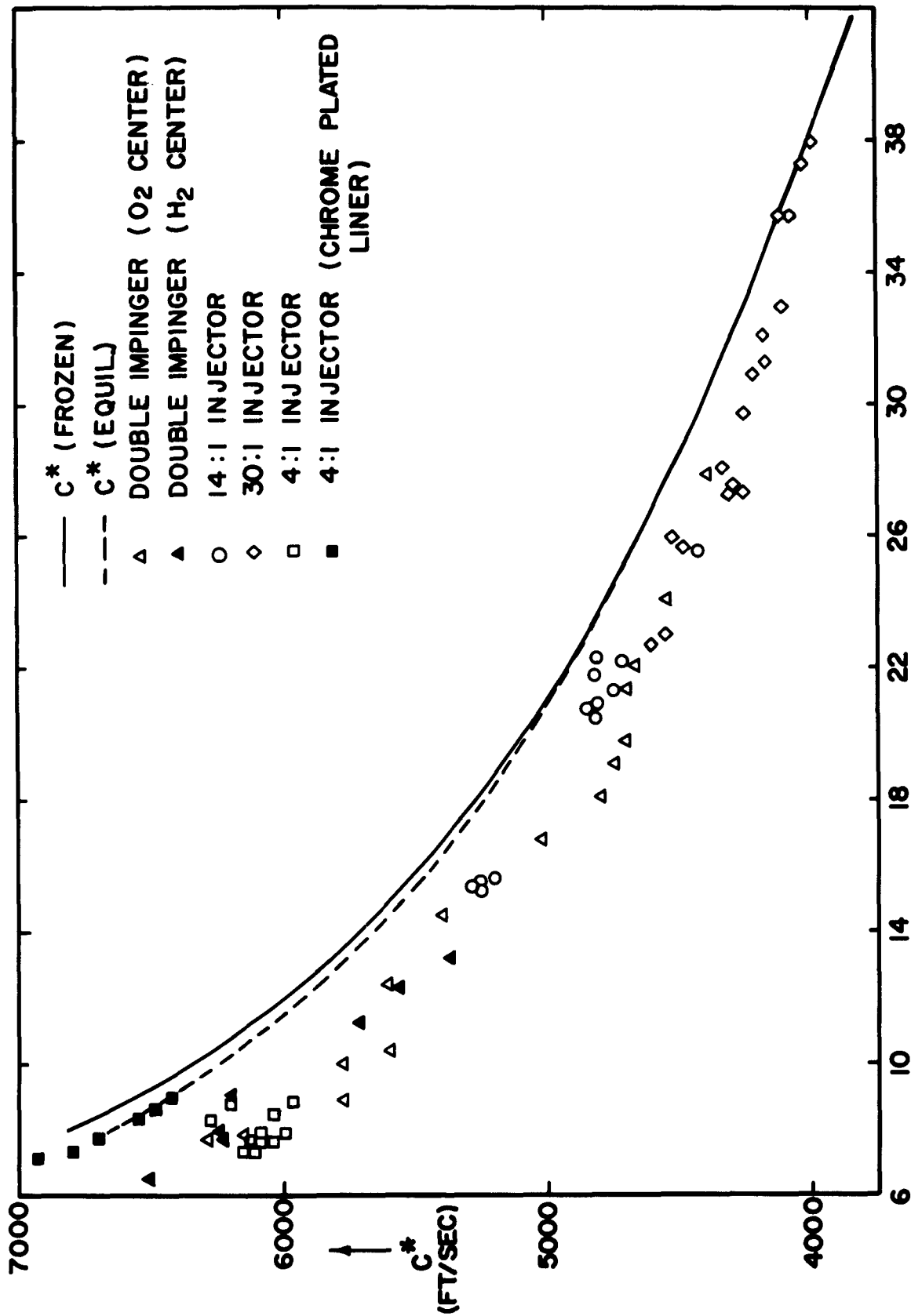


FIGURE 3: COMPARISON OF EXPERIMENTAL AND CALCULATED  $C^*$

when any injector was used outside its designed range, did the efficiency drop below 90%. In these cases the spectroscopically determined exit temperatures were significantly below the values observed which were obtained running with more efficient injectors. In all cases, the final experimental emissivities were obtained only with injectors which are most efficient at the desired mixture ratio.

## EXPERIMENTAL MEASUREMENTS, RESULTS AND DISCUSSION

Temperature - The experimental determination of the temperature of the exit gas is necessary in order to evaluate the spectral emissivities and to determine the concentration of the  $H_2O$  in the sample from a semi-empirical fit to the experimental temperatures of a thermochemical flow calculation. The temperature of the gas jet was determined using a method similar to the one employed by Silverman in a study of the  $CO + O_2$  flames<sup>8</sup>. This method has been very successful when it was previously applied to temperature measurements of a kerosene-oxygen exhaust jet<sup>4</sup>.

The measurements of the exit temperatures have been made at different spectral regions in the 2.7 micron  $H_2O$  band from accurate transmission and emission measurements of the exit hot gas sample. The emissivity is calculated from the measured transmission with

$$\epsilon(\bar{\nu}) = 1 - \frac{I(\bar{\nu})}{I_o(\bar{\nu})} ,$$

where  $I_o(\bar{\nu})$  = incident global energy, and  $I(\bar{\nu})$  = transmitted energy of global attenuated by the exit gas. The temperature is determined from the corresponding blackbody energy:

$$W(\bar{\nu}, T_R) = \frac{J(\bar{\nu})}{\epsilon(\bar{\nu})} ,$$

where  $W(\bar{\nu}, T_2) = C_1 \bar{\nu}^3 \left[ 1 - \exp\left(-\frac{C_2 \bar{\nu}}{T_R}\right) \right]^{-1}$ ,  $J(\bar{\nu})$  = emitted energy from hot exit gases, obtained from a comparison with a standard blackbody calibration source and  $C_1$  and  $C_2$  are the radiation constants. The results of the experimental temperatures as a function of the mixture ratio ( $O_2/H_2$  by weight) are shown in Fig. 4. It should be noted that experimental measurements were made only on the oxygen rich side of stoichiometric because the temperature is relatively insensitive to mixture ratio in this region.

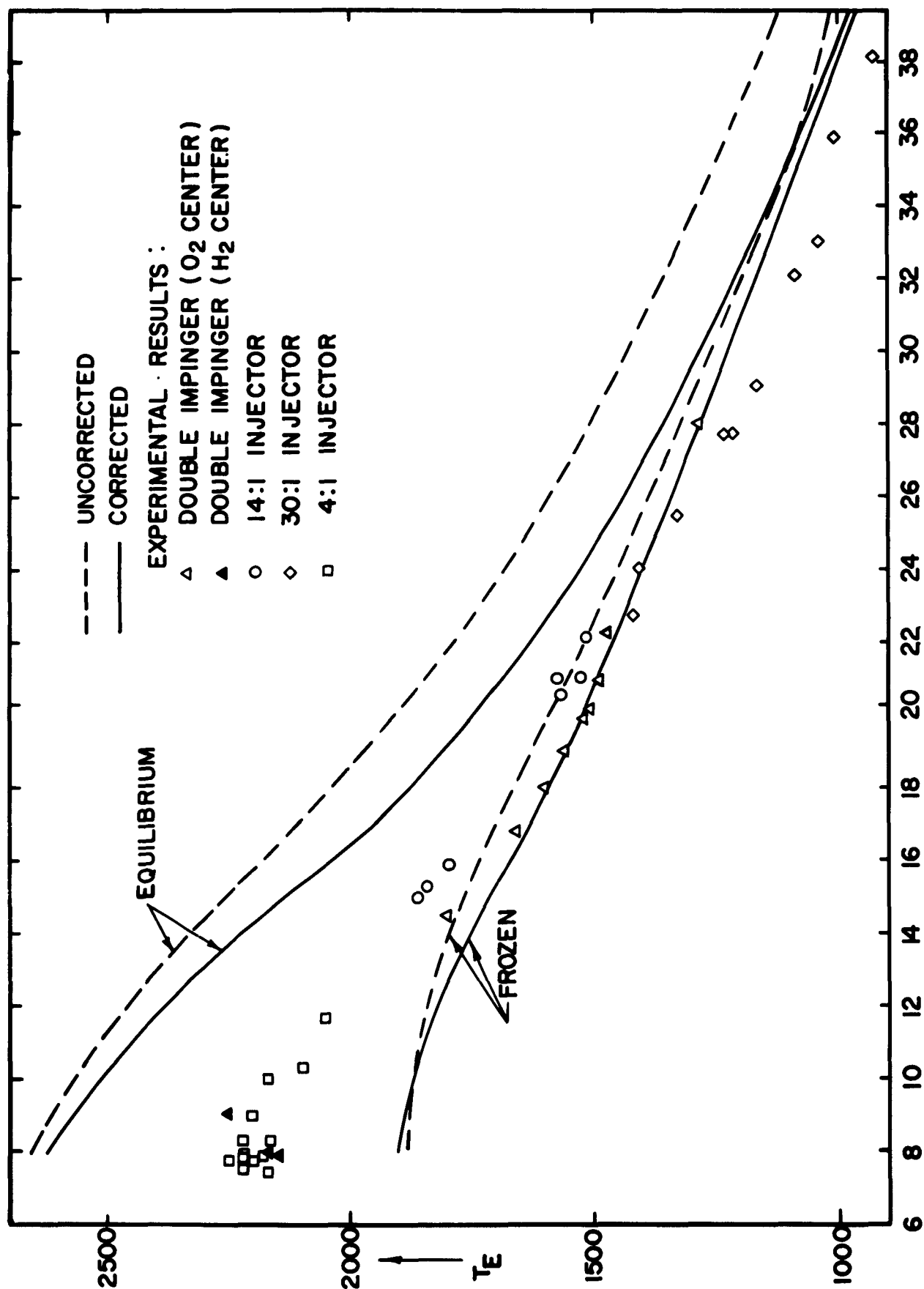


FIGURE 4: CALCULATED AND EXPERIMENTAL EXIT TEMPERATURES

Compositions - The temperature and composition of the balanced exhaust jet have been calculated with the "PEEP" thermochemical computer program for the two limiting cases of frozen equilibrium and shifting equilibrium. "Frozen" means that the composition does not change during the expansion in the burner nozzle while "shifting" means that the composition changes during the expansion and adjusts to the temperature. The chamber pressures needed for the calculation have been obtained during the experiments. The mean deviation of  $\pm 2\%$  in chamber pressure per individual injector has a negligible effect on the calculated parameters.

The rocket burner is water cooled during its operation and a constant temperature rise has been observed during the experiment. Heat, then has been transferred from the combustion gas to the burner walls. An attempt has been made to correct for the heat loss to the coolant. The enthalpy amounts to 44.8 kcal/sec for an average water flow of 5.9 lbs/sec and a temperature difference of 30°F. This amount of heat loss was approximately the same regardless of mixture ratio. By dividing the enthalpy loss by the experimentally determined mass flow of the fuel, the enthalpy loss in kcal/mole fuel is obtained for the different mixture ratios. Since the coolant surrounds the injector face, the chamber, the throat, and the expansion nozzle, the heat is transferred over the entire liner in an unknown manner. It appears to be rather difficult to make a detailed analysis, involving a non-isentropic expansion in the nozzle. As a first approximation, the isentropic expansion is retained and the heat transfer is limited to the chamber (non-adiabatic combustion). However, since the highest heat transfer would take place in the throat and would reduce the temperature of the non-isentropically expanding exit gases even more, the approximation does not yield a lower limit.

The calculated exit temperatures with and without corrections for the heat loss versus mixture ratios are plotted in Fig. 5. The calculated mole fractions of  $H_2O$  and OH are shown in Fig. 6. The difference between the uncorrected and corrected concentrations is very small at stoichiometric conditions and becomes negligible at leaner mixture ratios.

The spectroscopically determined exit temperatures which are shown in Fig. 4 have been used to determine the actual concentrations by means of a shifting changing to frozen thermochemical flow model. It should be pointed

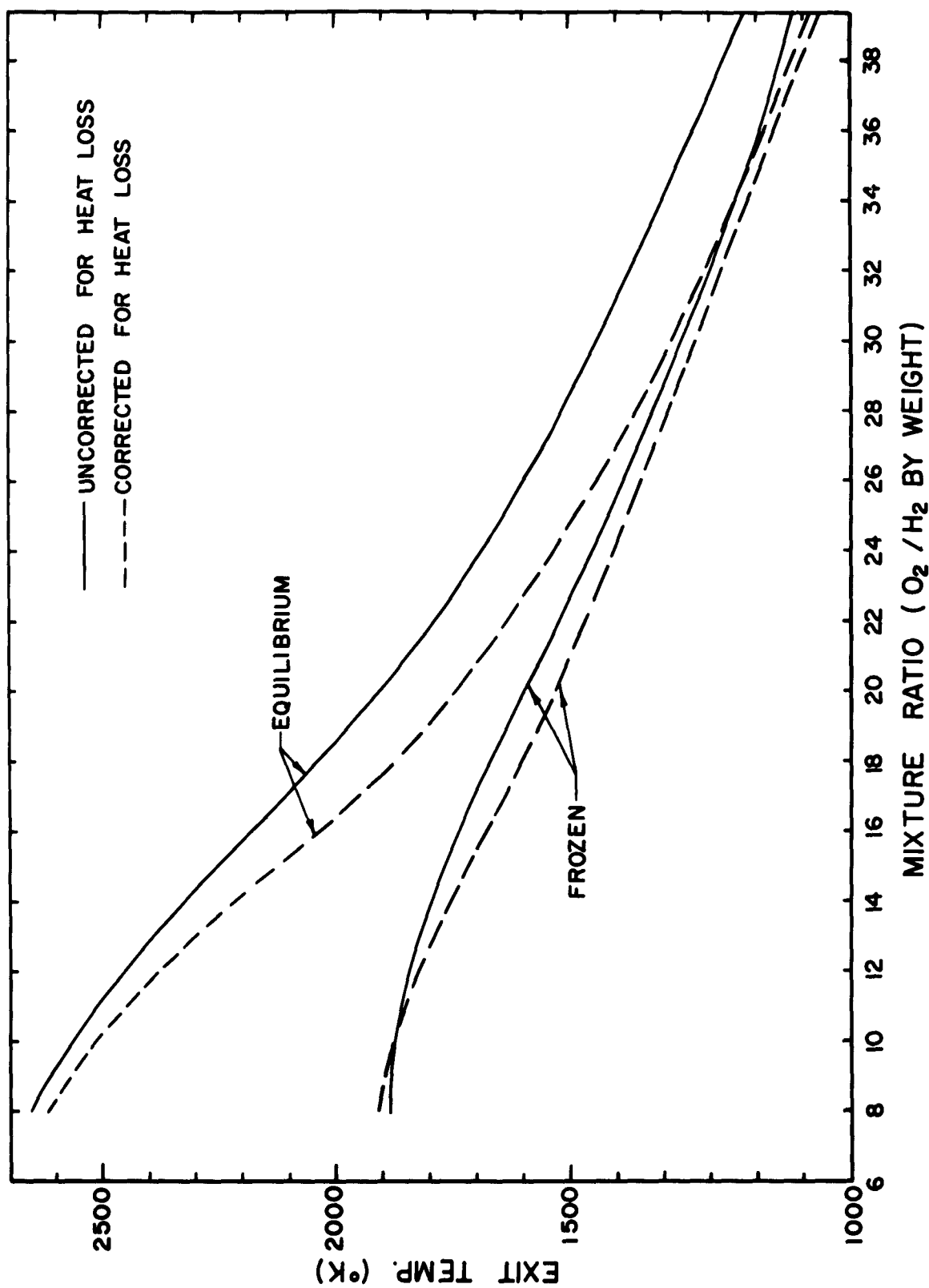


FIGURE 5: EXIT TEMPERATURE CORRECTED FOR HEAT LOSS

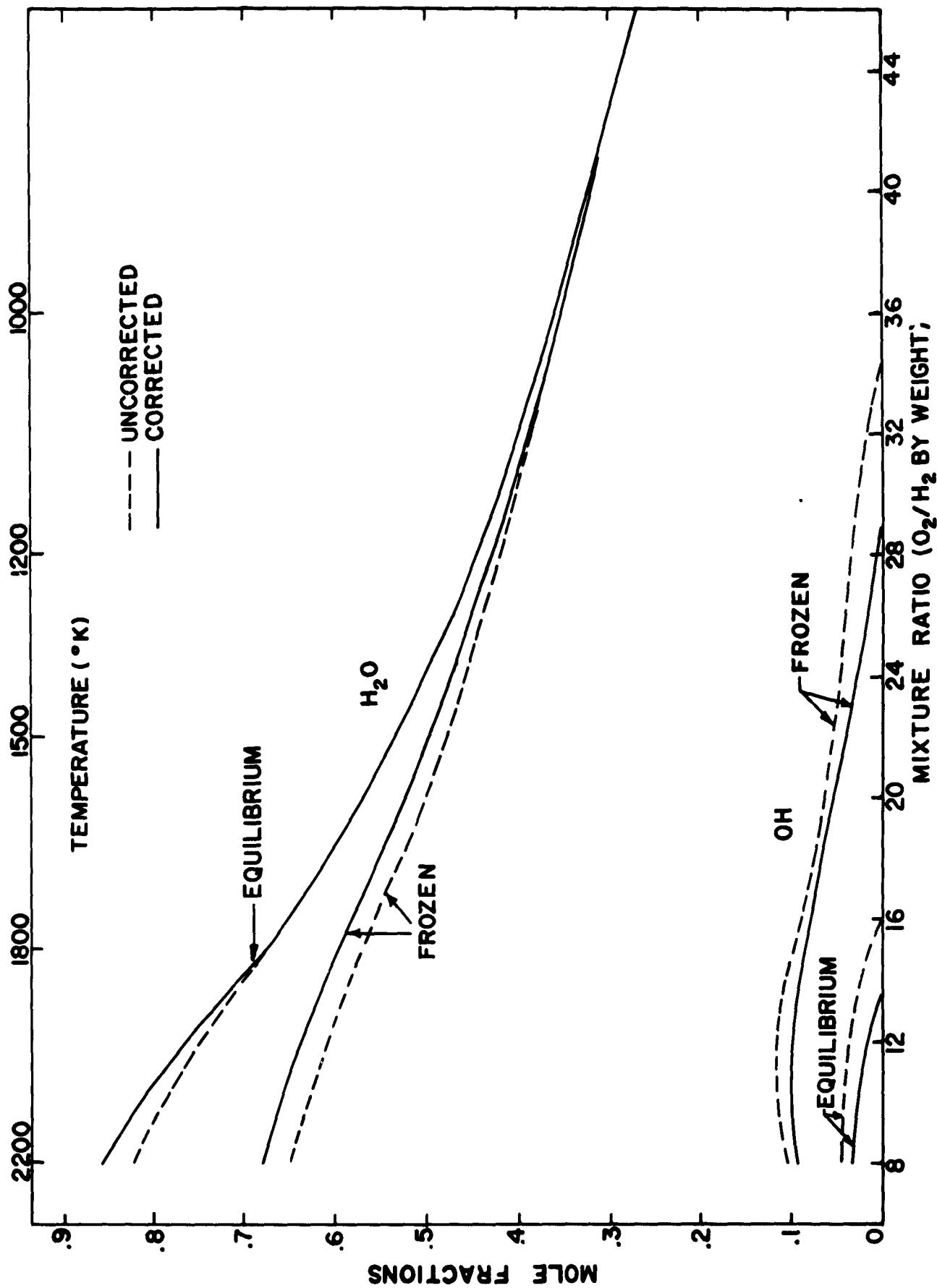


FIGURE 6: COMPOSITION OF EXIT GAS VERSUS TEMPERATURE



out that the first approximation for correcting the heat loss does change the theoretical exit temperatures very little at the high temperatures, where the uncertainty of the concentrations is large (20%). On the other hand, the exit temperatures are lowered considerably at leaner mixture ratios by the first approximate correction where the uncertainty of the concentrations is smaller. Thus, it appears that a better approximation in correcting the heat loss would probably not result in a more accurate determination of the concentrations. Therefore, the uncertainties in the concentrations are given within the experimental spread of the temperatures at the fuel rich mixture ratios. At the leaner mixture ratios where the experimental temperature data fall outside the calculated ones, the concentrations are given within the limits of the frozen and shifting equilibrium cases. The experimental errors in the exit temperature have been determined by a least square curve fits. The errors amount to  $\pm 1.6\%$ . The uncertainties in partial pressure of  $H_2O$  for the fuel rich mixture ratios are

$$\Delta p = \frac{\Delta T}{(T_{\text{equ}} - T_{\text{Froz}})} (P_{\text{equ}} - P_{\text{Froz}}),$$

and for the lean mixture ratios

$$\Delta p = (P_{\text{Equ}} - P_{\text{Froz}}),$$

which results in an average error of  $\pm 1.5\%$ . Since the geometrical depth is known within  $\pm 1.5\%$ , the total error in optical depth  $pl$  is  $\pm 3\%$ . A graph of  $(pl)$  of  $H_2O$  and  $OH$  versus mixture ratios and temperature is given in Fig. 7. In some presentations, the optical depth in  $(\text{cm-atm})_{\text{STP}}$  is used:

$$u = \frac{P_{H_2O}}{P_o} \frac{T_o}{T} l (\text{cm-atm})_{\text{STP}}$$

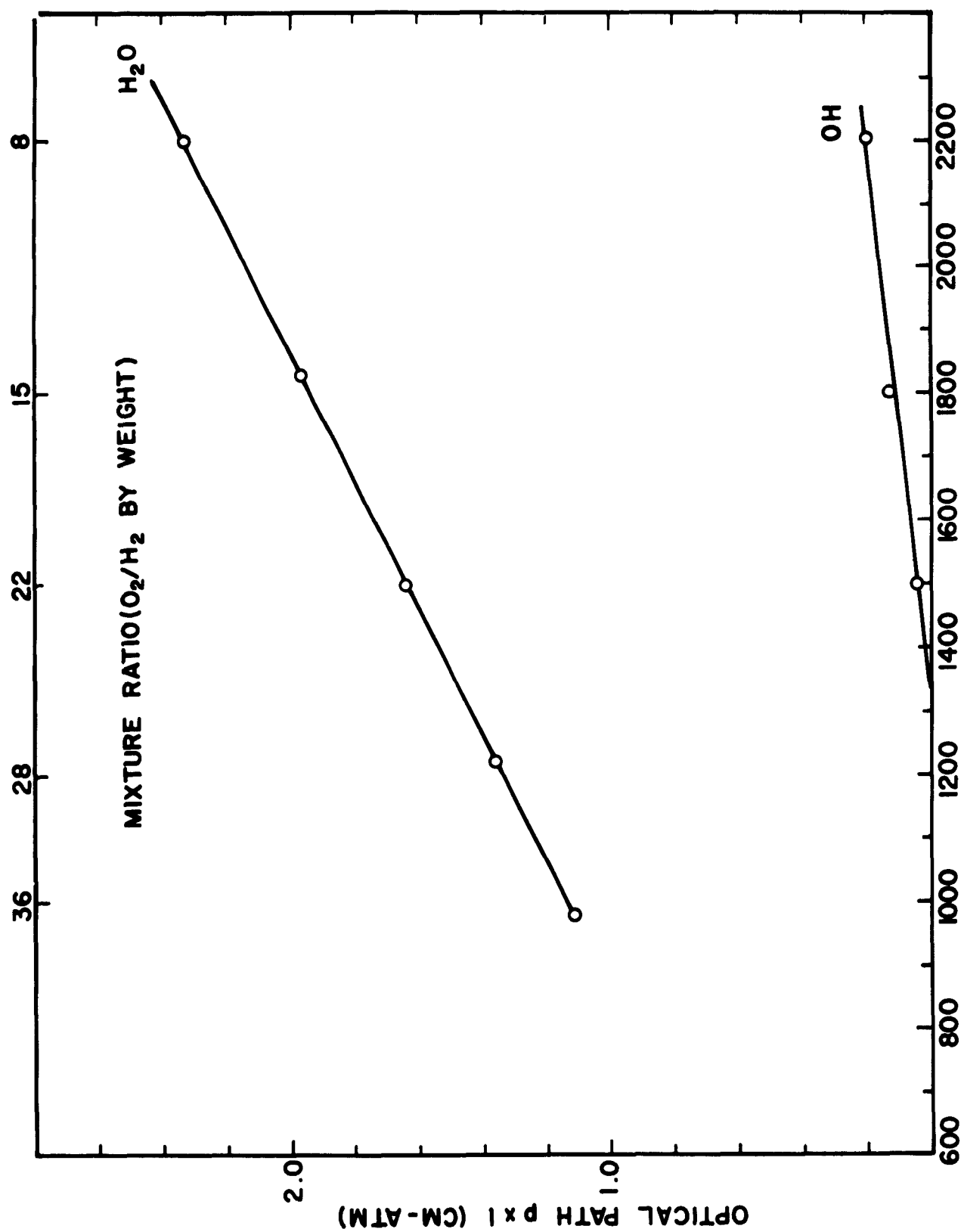


FIGURE 7: OPTICAL DEPTH OF  $\text{H}_2\text{O}$  AND  $\text{OH}$  IN SAMPLE

where  $T_0 = 273^\circ\text{K}$ ,  $p_0 = 1 \text{ atm}$ ,  $T = \text{exit temperature}$ , and  $l = 3.12 \text{ cm}$ . To convert  $u$  into precipitable cm, it must be multiplied by  $\rho_0(\text{H}_2\text{O}) = 8.041 \times 10^{-4} \text{ g/cc}$ . In these experiments, the value of  $u$  is constant for all temperatures. It is  $u = 0.30 (\text{cm-atm})_{\text{STP}} \pm 3\%$ , or  $2.41 \times 10^{-4} \text{ gm/cm}^2$ .

Spectral Emissivities - The measurements of the emissivities were made by determining the spectral energy emitted from the burner exit gas and dividing by the blackbody energy at the particular wave number and temperature. The following equation which expresses the spectral emissivity,  $\epsilon(\bar{\nu}, T_R)$ , in terms of the spectral radiance of the hot gas  $J(\bar{\nu})$  and spectral radiance of the blackbody,  $W(\bar{\nu}, T_R)$  was used:

$$\epsilon(\bar{\nu}, T_R) = \frac{J(\bar{\nu})}{W(\bar{\nu}, T_R)} ,$$

where  $T_R$ , the temperature hot gas sample at the appropriate mixture ratio, is taken from the best fit to the experimental values shown in Fig. 4. The appropriate optical depth is then found from Fig. 7. The emitted energy is obtained on an absolute basis by relating the instrument deflection to a standard blackbody, the temperature of which is determined with a Pt-Rh thermocouple. Readings from the traces (burner and blackbody emission) are made at constant micrometer drum readings of the spectrometer and serve as input to a 650 data reduction program. The conversion of micrometer drum readings into wavenumbers is made with a 4-point interpolation procedure based on the original wavenumber calibration. The wavenumber intervals, at which the readings were taken, are  $9 \text{ cm}^{-1}$  at  $2800 \text{ cm}^{-1}$  and  $15 \text{ cm}^{-1}$  at  $4400 \text{ cm}^{-1}$ . The computer output consists of a listing (on cards) of wavenumbers in  $\text{cm}^{-1}$ , wavelength in  $\mu$ , the energy radiated by the exhaust gases in  $\text{watts/cm}^2$ , and the emissivity. The listings for five different runs (at  $T = 1000, 1200, 1500, 1800$  and  $2200^\circ\text{K}$ ) are reproduced in the Appendix. The emissivity spectra for the  $2.7 \text{ micron}$ ,  $\text{H}_2\text{O}$  band at  $1000, 1200, 1500, 1800$  and  $2200^\circ\text{K}$  are shown in Figs. 8 through 12, respectively. Since the observations were made at constant spectrometer drum readings and not at constant wavenumber increments, not all

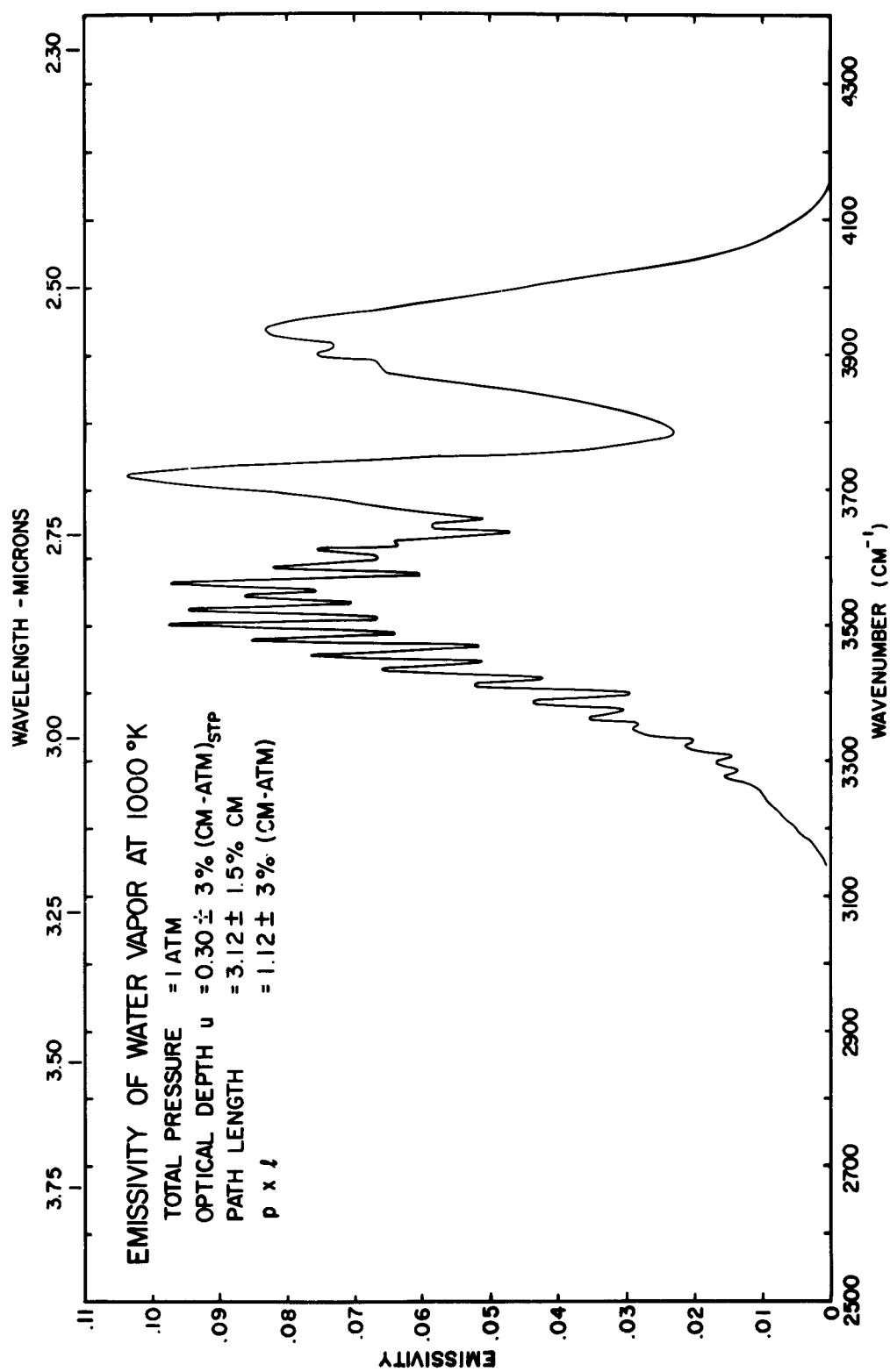


FIGURE 8: EMISSIONITY OF H<sub>2</sub>O AT 1000°K WITH 12 cm<sup>-1</sup> SPECTRAL SLIT

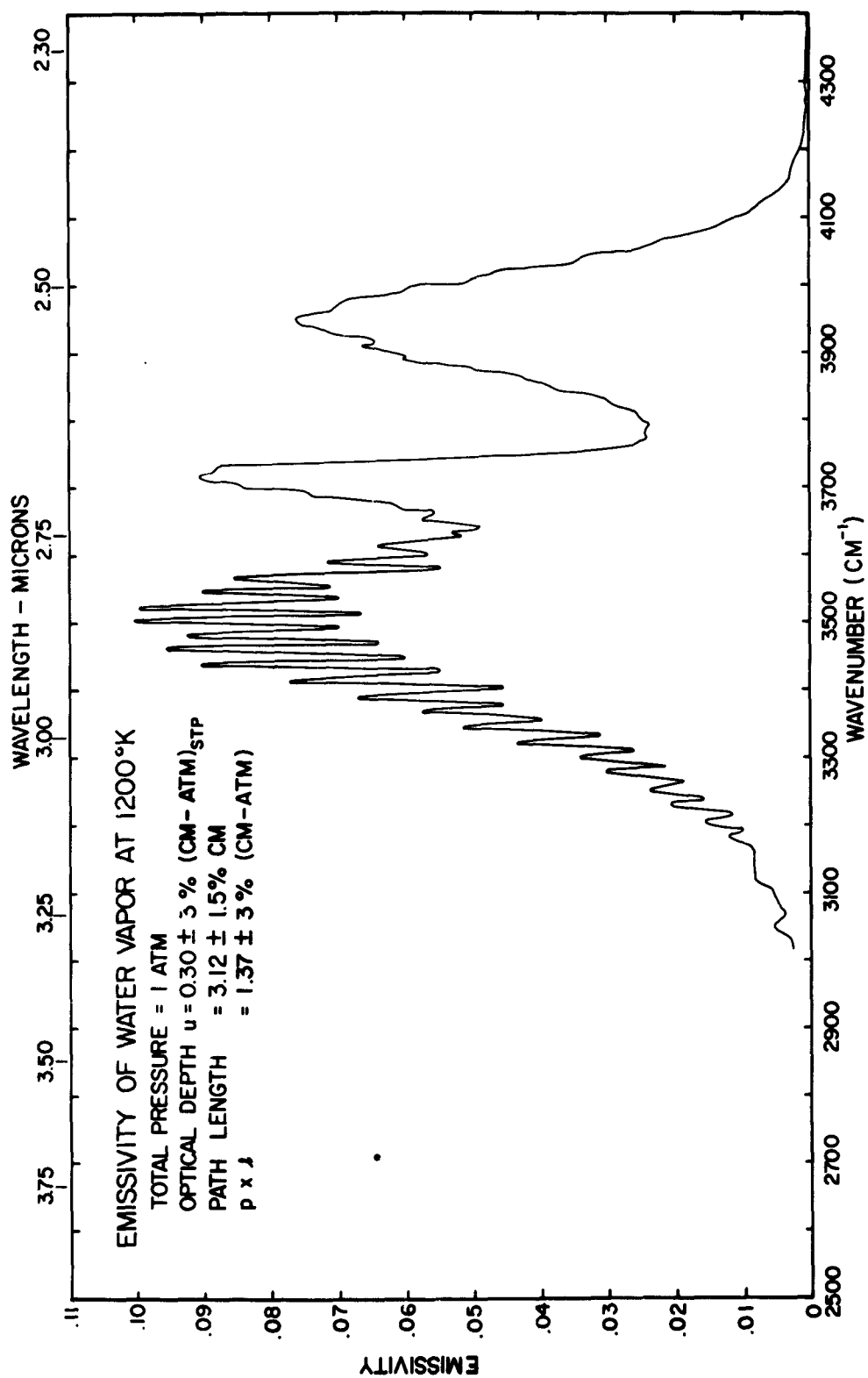


FIGURE 9: EMISSION OF H<sub>2</sub>O AT 1200°K WITH 12 cm<sup>-1</sup> SPECTRAL SLIT

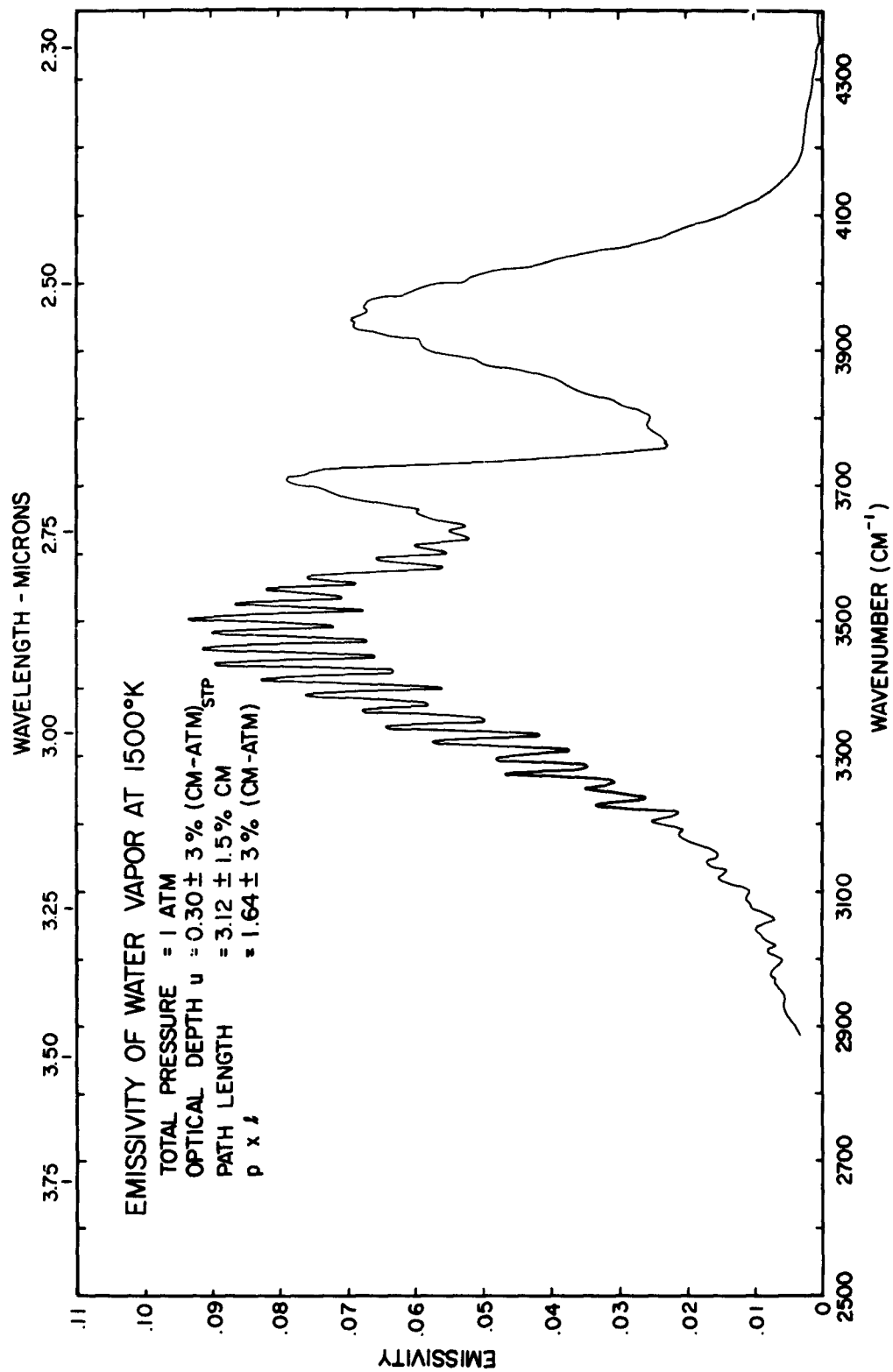


FIGURE 10: EMISSIONITY OF  $H_2O$  AT 1500°K WITH 12  $CM^{-1}$  SPECTRAL SLIT

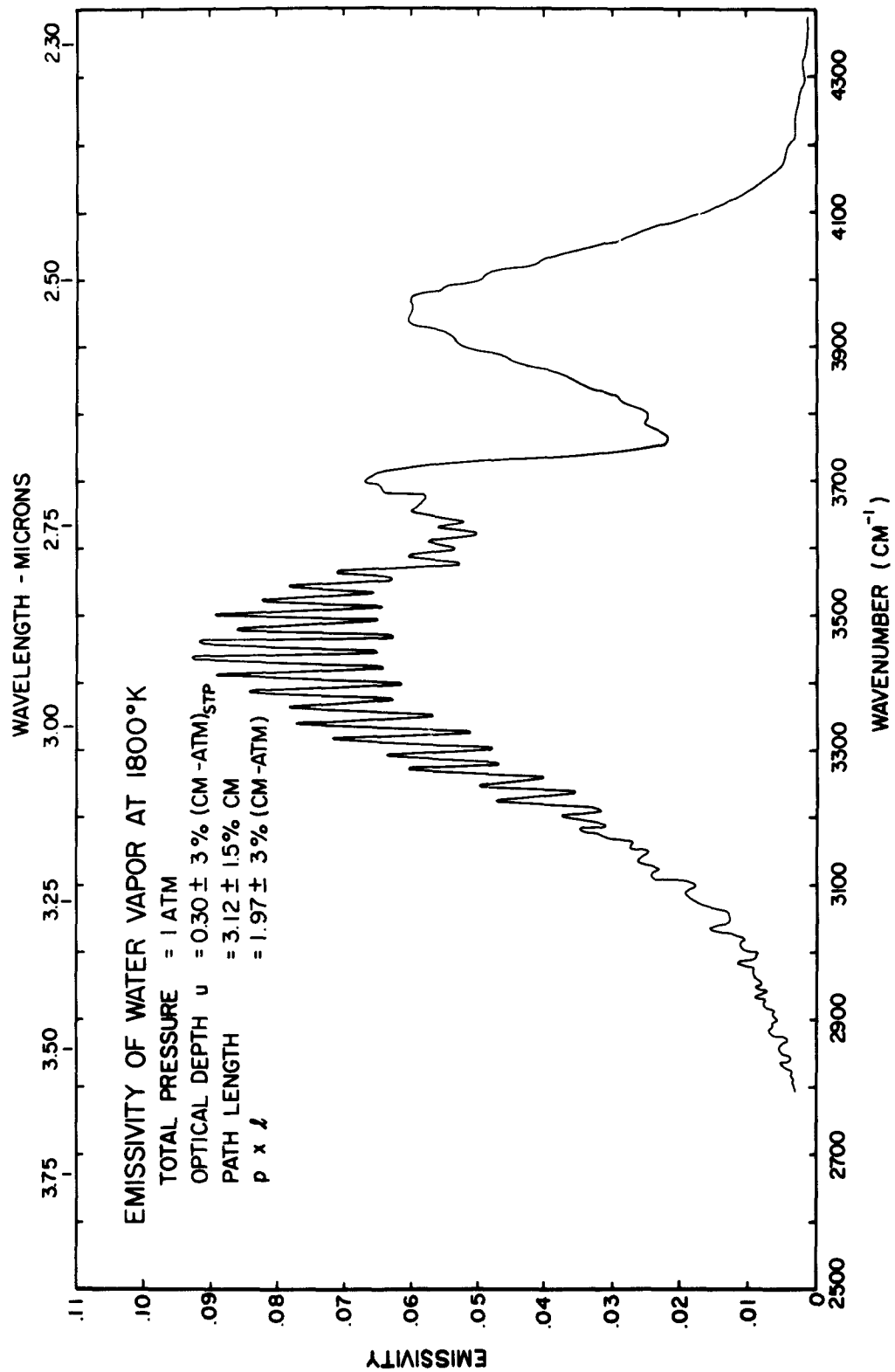


FIGURE 11: EMISSION OF  $\text{H}_2\text{O}$  AT 1800°K WITH 12  $\text{cm}^{-1}$  SPECTRAL SLIT

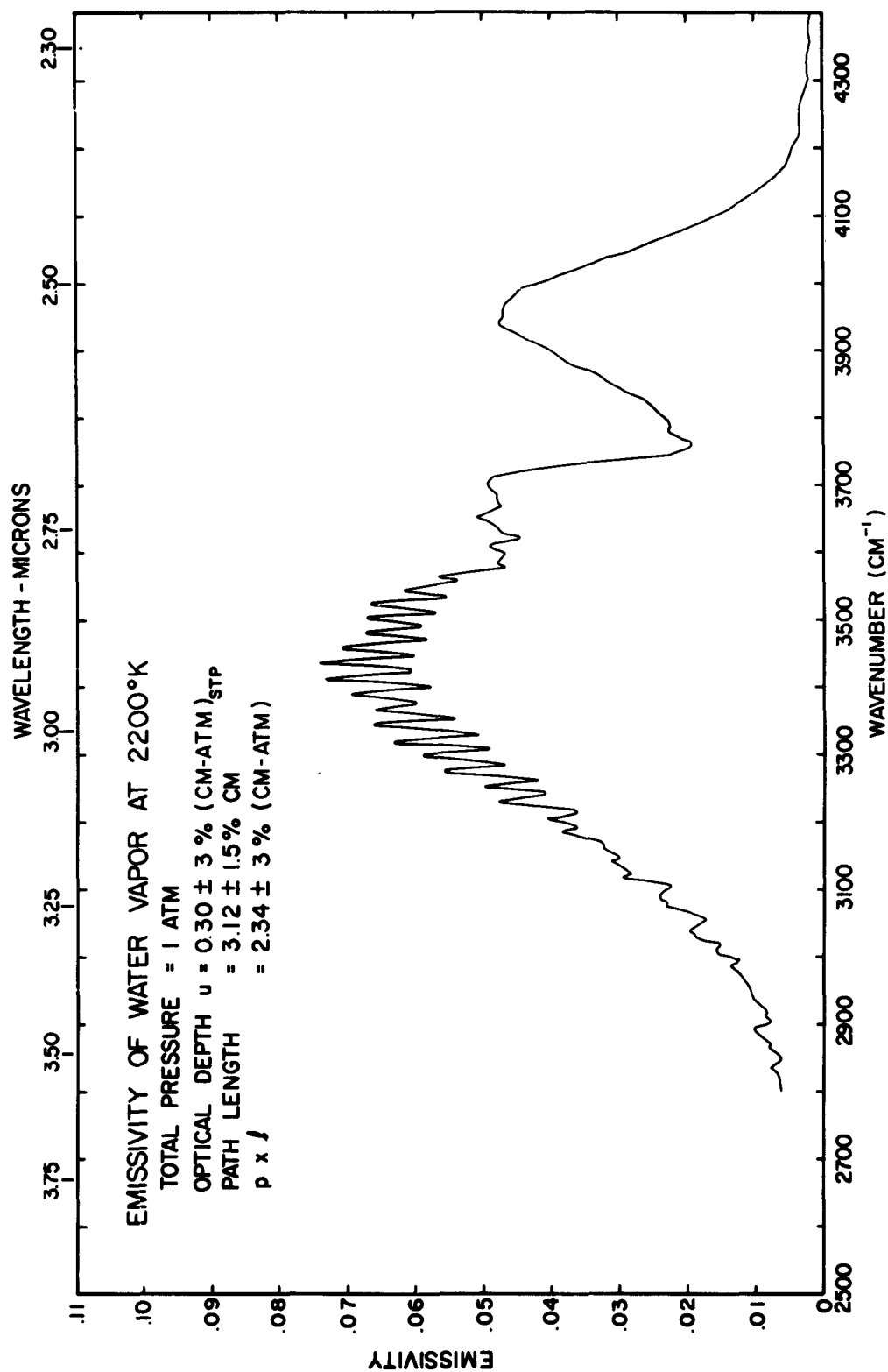


FIGURE 12: EMISSIONITY OF H<sub>2</sub>O at 2200°K WITH 12 cm<sup>-1</sup> SPECTRAL SLIT



of the peak maxima and minima were covered and hand calculations for these points were made.

In order to compare the emissivities and show the temperature variation, an averaged composite of all the previous emissivity curves was made by smoothing out the structure. The comparison is shown in Fig. 13 and shows the temperature variation very nicely. The spectra in Figs. 8 through 12 were smoothed by taking the mean value of the two envelopes of the maxima and minima. In order to check this averaging procedure the total band area,  $\int \epsilon(\bar{\nu}) d\bar{\nu}$ , under the smoothed curves was compared with the detail emissivity plots as determined with a planimeter; no difference was observed.

These integrations were also used to give the apparent integrated band intensity,  $\bar{\alpha} \text{ (cm}^{-2}\text{atm}^{-1}\text{)}_{\text{STP}}$  at different temperatures of the 2.7 micron  $\text{H}_2\text{O}$  band. The apparent integrated intensity is then defined as:

$$\bar{\alpha}_{\text{STP}} = \frac{1}{u} \int_{\text{band}} \ln\left(\frac{1}{1-\epsilon}\right) d\bar{\nu}$$

The error in replacing  $\ln \frac{1}{1-\epsilon}$  by  $\epsilon$  is proportional to  $\frac{\epsilon}{2} \times 100\%$  for  $\epsilon \leq 0.1$ . The error for the integral is about 3%. The values listed for  $\bar{\alpha}$  in Fig. 13 are corrected by this amount. The integrated band intensity of the  $\text{H}_2\text{O}$  band will be discussed in a later paragraph.

In Fig. 14 the "apparent absorption coefficient",

$$k(\bar{\nu}) = \frac{\ln \frac{1}{1-\epsilon}}{u} \text{ (cm}^{-1}\text{atm}^{-1}\text{)}_{\text{STP}},$$

as a function of the temperature for various spectral regions are shown. The apparent absorption coefficient is implicitly a function of the concentration of  $\text{H}_2\text{O}$ , total pressure and geometrical path; however, the results in Fig. 14 do show the qualitative behavior since all of the aforementioned parameters were constant in the present experiments.

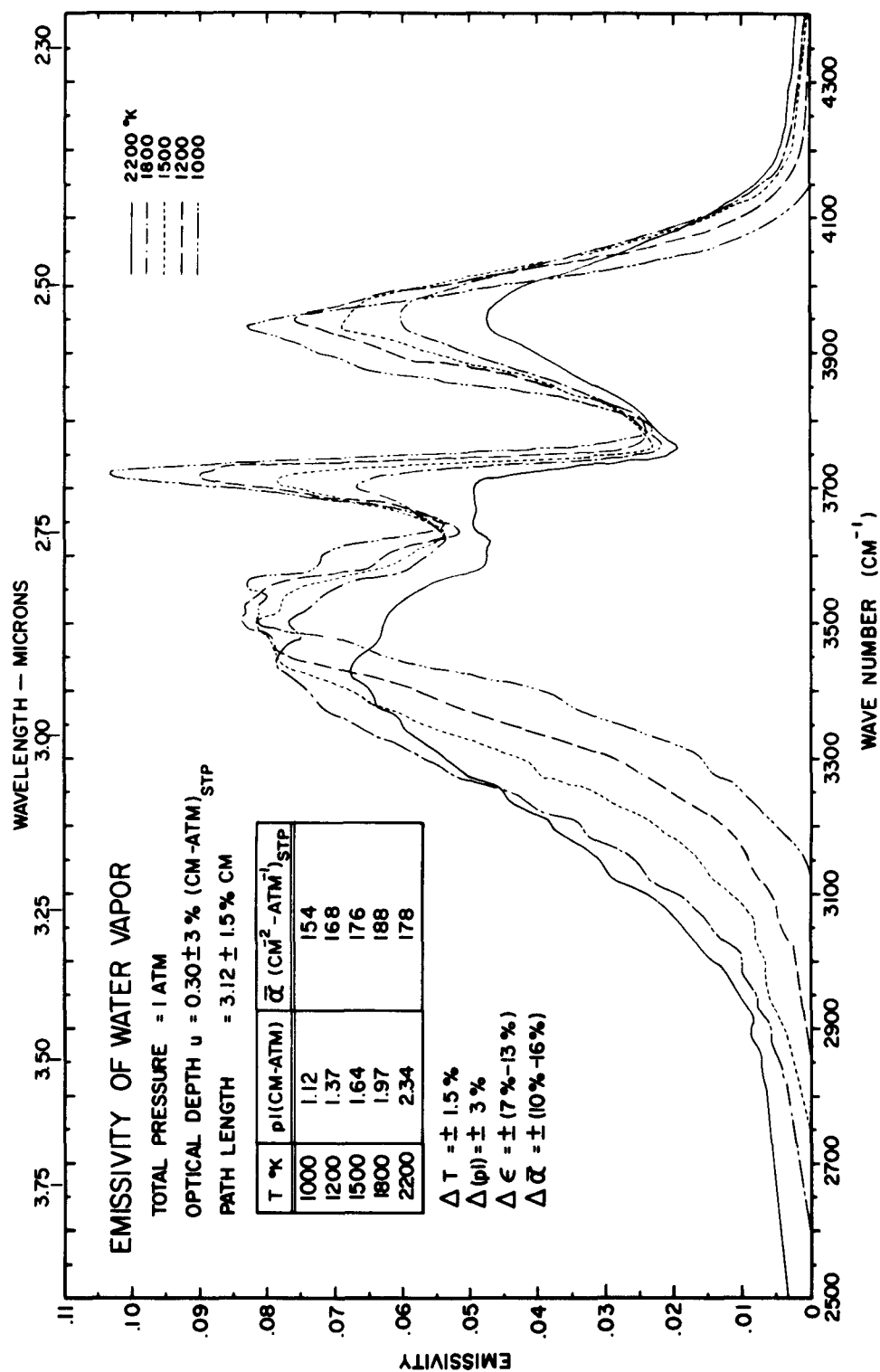


FIGURE 13: AVERAGED EMISSIVITIES VERSUS TEMPERATURE

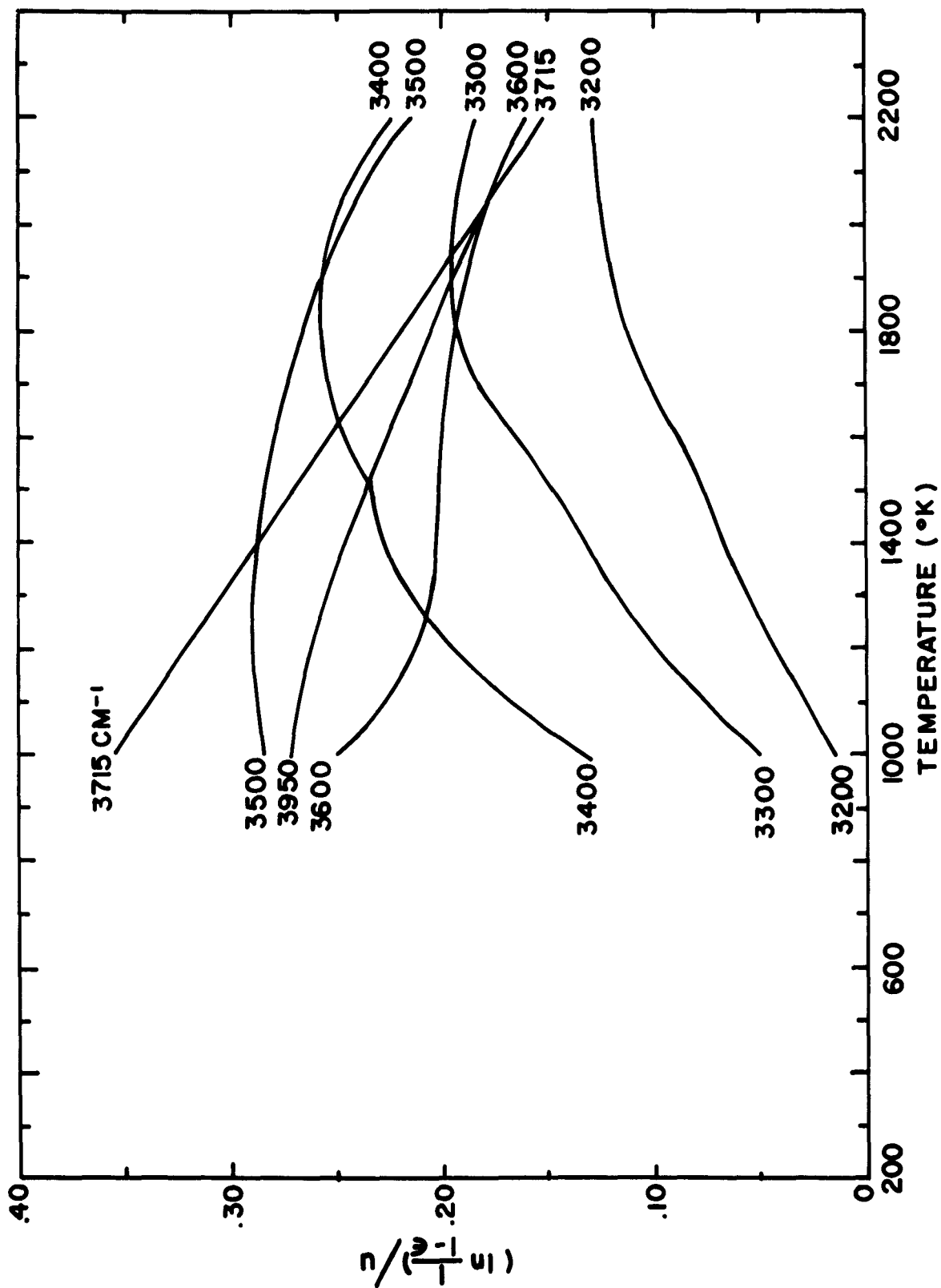


FIGURE 14: COMPARISON OF APPARENT SPECTRAL ABSORPTION COEFFICIENTS

A detailed analysis of the errors in the emissivities shows that the main contribution is in the uncertainty of the temperature of the exhaust gases:

$$\frac{d\epsilon}{\epsilon} = \frac{C_2}{T^2} \bar{\nu} \left(1 + \frac{W(\bar{\nu}, T)}{C_1 \bar{\nu}^3}\right) dT$$

where  $C_1$  and  $C_2$  are the constants in the blackbody function  $W$ ,  $\bar{\nu}$  = wavenumbers,  $T$  = gas temperature. The other errors (calibration, reading, etc.) at reasonable deflections are constant and amount to  $\pm 3.6\%$ . A plot of the uncertainties in  $\epsilon$  versus temperature (with wavenumbers as parameters) is given in Fig. 15. For very low deflections, the errors are somewhat higher.

An additional uncertainty in emissivities at the higher temperatures is caused by the small amount of OH present in the sample. According to the calculations, there is about 10% OH of the water concentration at stoichiometric conditions, becoming less toward leaner mixture ratios (see Fig. 6). An attempt has been made to correct for the contribution of OH to the emissivities. The absorption coefficient in the weak line approximation<sup>9</sup> times the  $p\ell$  is shown in Fig. 16. The corrections to the individual emissivities are within the experimental uncertainties and were not made; however, the OH correction to the integrated band intensity was made in an attempt to improve the accuracy of the intensity results.

For the present conditions, the integrated emissivities of OH are approximately  $2.0 \text{ cm}^{-1}$ ,  $2.1 \text{ cm}^{-1}$  and  $0.1 \text{ cm}^{-1}$  for  $T = 2200^\circ\text{K}$ ,  $1800^\circ\text{K}$  and  $1500^\circ\text{K}$ , respectively. At lower temperatures, the correction vanishes. It is now possible, to correct the integrated emission of the water vapor band,  $\int \epsilon(\bar{\nu}) d\bar{\nu}$ , by these amounts. In the following table, the corrected and uncorrected values for the integrated absorption for the 2.7 micron water vapor band are given:

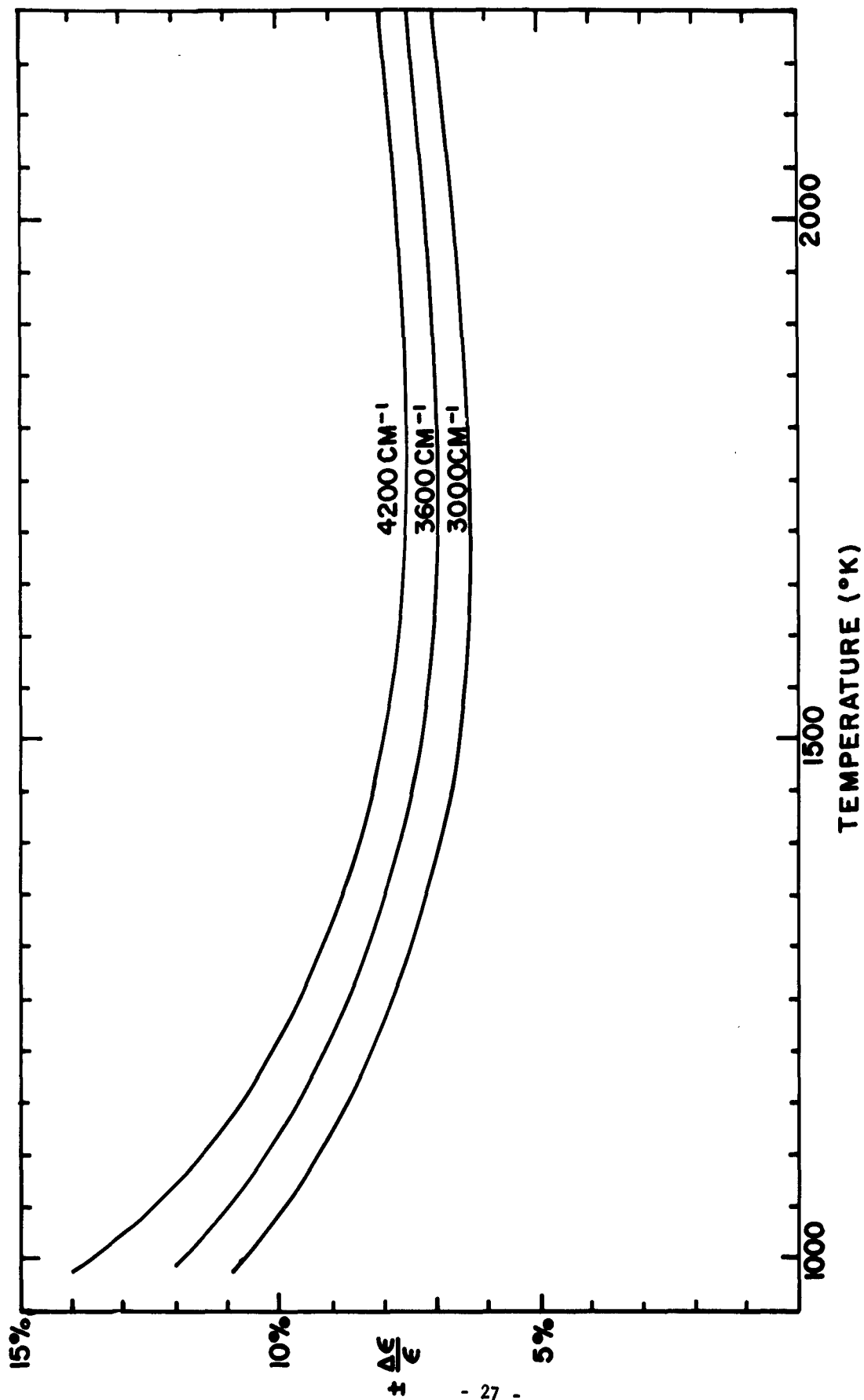


FIGURE 15: EMISSIVITY ERRORS VERSUS TEMPERATURE

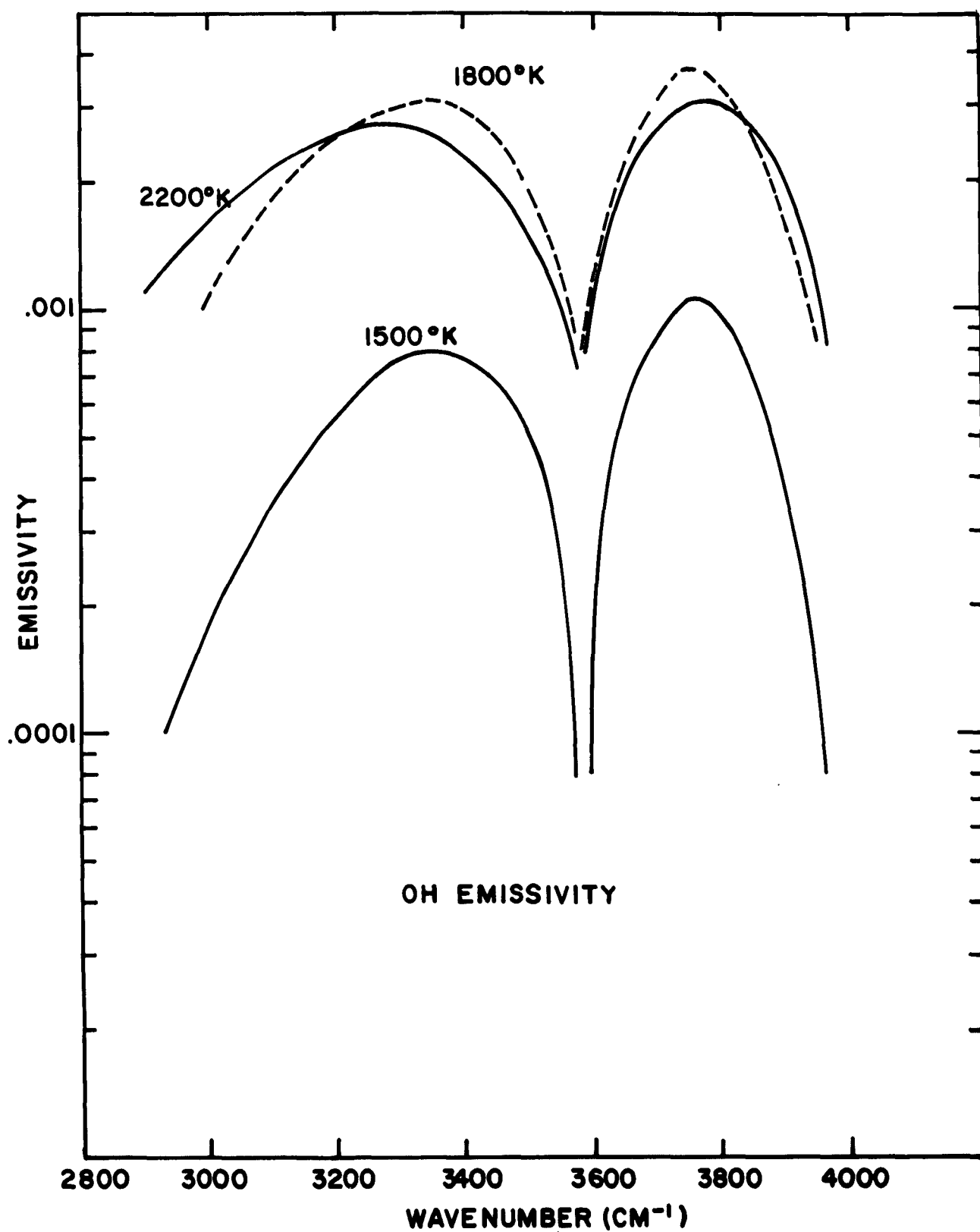


FIGURE 16: EMISSIONITY OF OH AT VARIOUS TEMPERATURES

T°K	1000	1200	1500	1800	2200
$\alpha_{\text{uncorr.}}$	$154 \pm 16\%$	$168 \pm 13\%$	$176 \pm 11\%$	$188 \pm 10\%$	$178 \pm 11\%$
$\alpha_{\text{corr}}$	154	168	176	182	171

The error values are taken from Fig. 15, plus an additional 3% from the uncertainty in the optical path.

Integrated Intensities - The apparent integrated intensity of the 2.7 micron  $\text{H}_2\text{O}$  band has been determined at more temperatures than shown in Fig. 12. The results of all the intensity measurements as a function of temperature corrected for the OH contribution are shown in Fig. 17 together with comparable results taken from the work of Burch, et al.<sup>2</sup>. The curve shows that the intensity values do decrease as the temperature is reduced which indicates that the band at lower temperatures does not act like it is "pressure broadened". There is some evidence to believe that at the high temperature at least, the band is sufficiently smeared, or essentially statistical because of the present small emissivities. The assumption implies that the apparent integrated intensity evaluated in the present work,  $180 (\text{cm}^{-2} \text{atm}^{-1})_{\text{STP}}$ , is a good approximation to the absolute band intensity of the 2.7 micron  $\text{H}_2\text{O}$  band. The results also show that the integrated intensity does not markedly vary as a function of temperature. There is some reason to believe that the integrated intensity of this fundamental band does not vary with temperature.

#### ACKNOWLEDGEMENTS

The authors wish to acknowledge the great assistance of Carlos N. Abeyta in the study, C. A. Sheen and D. Suttie of the General Dynamics/Convair, Thermodynamics Laboratory for running the rocket burner, and Dr. J. A. L. Thomson for his helpful discussion.

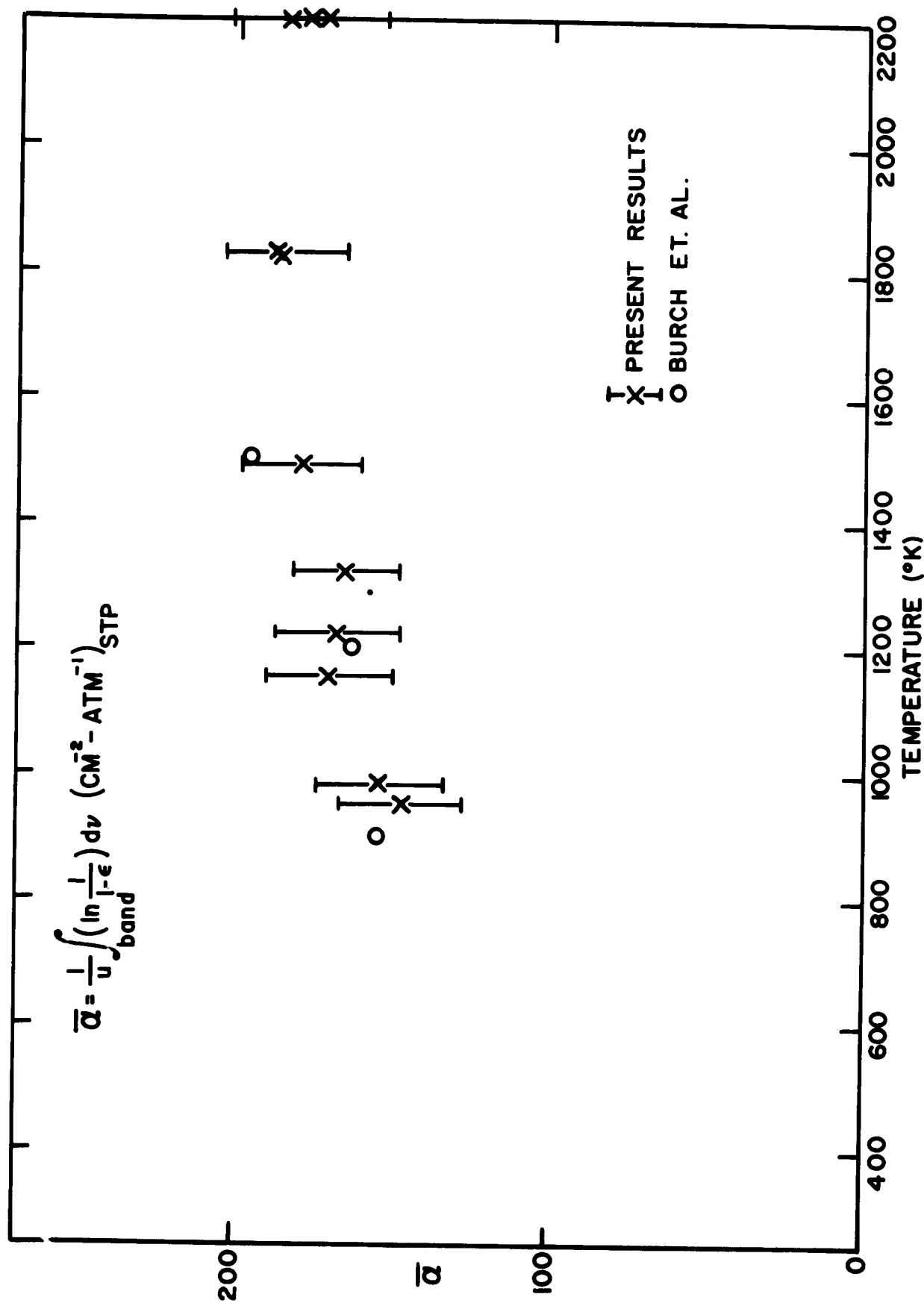


FIGURE 17: APPARENT INTEGRATED INTENSITIES VERSUS TEMPERATURE



## REFERENCES

1. J. N. Howard, D. E. Burch, and D. Williams, J. Opt. Soc. Am., 46, 242 (1956).
2. D. E. Burch and D. A. Gryvnak, Report No. V-1929, Ford Motor Company, Aeronutronics Division, Newport Beach, California, October, 1962.
3. R. H. Tourin, J. Opt. Soc. Am., 51, 799 (1961).
4. C. C. Ferriso, J. Chem. Phys., 37, 1955 (1962).
5. C. C. Ferriso, Report No. AE61-0910, General Dynamics/Astronautics, San Diego, California, September, 1961.
6. C. A. Skeen, Report to be published.
7. F. P. Boynton, III, private communication, General Dynamics/Astronautics, San Diego, California.
8. S. Silverman, J. Opt. Soc. Am., 39, 275 (1949).
9. W. Malkmus, Report No. ZPh-120, General Dynamics/Convair, San Diego, California, September, 1961.

## APPENDIX

The computer output listings are given in the following pages for the experiments performed at 1000°, 1200°, 1500°, 1800° and 2200°K. For the particular temperature, given in the upper right hand corner of the page, the output is given for:  $\bar{\nu}$ , wavenumber in  $\text{cm}^{-1}$ ;  $\mu$ , wavelength in microns; E, energy in watts per  $(\text{cm}^2 - \cancel{\text{m}^2})$ ; and  $\epsilon$ , the emissivity.

The entries are in 650 floating point and the last two numbers fix the decimal point.

3157565854 is .31575658 x  $10^4$  or 3157.5658

3166996650 is .31669966 x  $10^0$  or .31669966

1288473348 is .12884733 x  $10^{-2}$  or .0012884733

$\bar{\nu}$	$\mu$	$\varepsilon$	$\epsilon$	1000°K
3115478654	3209779751			
3121800054	3203280251			
3127307154	3197639351			
3133324554	3191498451			
3139500054	3185220651			
3145397254	3179248751			
3151367154	3173226051			
3157565854	3166996651	1288473348	0001120451	
3164242354	3160314251	1927815648	0001675251	
3172972054	3151619451	2561829248	0002224351	
3179880054	3144772851	3193729248	0002771251	
3186385054	3138352751	3822748848	0003315151	
3192922854	3131926651	5083892748	0004406351	
3199494054	3125494251	5704479948	0004941551	
3206098354	3119056051	6347386248	0005495551	
3212735954	3112611951	6963459748	0006025851	
3219419754	3106149851	8207214648	0007098651	
3226139054	3099680551	8814242848	0007620051	
3232883554	3093213851	9417572548	0008137951	
3239652654	3086750751	1064323449	0009193151	
3246446454	3080291151	1123725649	0009702151	
3253265554	3073834651	1187590249	0010249551	
3260044554	3067442851	1246493649	0010753951	
3266839154	3061062951	1367154949	0011790751	
3273701154	3054646651	1672906649	0014422851	
3280630154	3048194951	1791417549	0015439751	
3287626454	3041708151	1607770549	0013852851	
3294690054	3035186951	1787699549	0015398851	
3301771854	3028676951	1966432049	0016934051	
3308922954	3022131551	1715125649	0014766451	
3316148354	3015546751	2268375849	0019525451	
3323448154	3008923251	2505281549	0021560451	
3330823054	3002261051	2375043549	0020436051	
3338272254	2995561651	3047080549	0026214651	
3345795954	2988825551	3340100549	0028731851	
3353394354	2982053151	3342121649	0028746251	
3361067354	2975245451	3935532249	0033847551	
3368814854	2968403051	4058655749	0034904551	
3376636954	2961526651	3560709949	0030621351	
3384533754	2954616851	4890355249	0042055751	
3392504954	2947674451	5051928849	0043446251	
3400550854	2940700151	3474567549	0029882551	
3408671454	2933694351	5392754549	0046383151	
3416910254	2926620751	5967565849	0051332651	
3425280954	2919468651	4953357849	0042614351	
3433656554	2912347251	7606863749	0065453551	
3442036954	2905256551	6923754149	0059587351	
3450422254	2898196151	6686900449	0057561851	
3458786754	2891187251	8817044549	0075917451	
3467165554	2884200451	6598988349	0056835251	
3475566754	2877228651	8424811949	0072583051	
3483990154	2870272251	9150318049	0078860251	
3492347854	2863403251	7475002749	0064445351	
3500566254	2856680751	1121192650	0096700251	
3508875754	2849915751	8313648949	0071733151	
3517276254	2843109151	8951500749	0077271451	
3525767854	2836261751	1093570050	0094444951	
3534349954	2829374651	8271434049	0071472151	
3543023654	2822448051	9959374549	0086104751	

1000°K

$\bar{\nu}$	$\mu$	E	$\epsilon$
3551787754	2815483651	8803928049	0076159751
3560643154	2808481451	1115730250	0096577951
3569740754	2801323951	8613588349	0076341751
3579073554	2794019251	7333066149	0063563451
3588378854	2786773851	9272024649	0080430851
3597657054	2779586851	7776250249	0067508251
3606908454	2772457451	8140285749	0070725951
3616132254	2765385651	7541280149	0065576551
3625328954	2758370451	7239787049	0063009651
3634004654	2751785251	5700489249	0049654851
3642661854	2745245251	6607236749	0057603551
3651713954	2738440251	6516733149	0056868151
3661160654	2731374351	6275665549	0054820151
3671101954	2723977851	7172465249	0062723251
3682048754	2715879351	8051096249	0070495451
3692864054	2707925351	8821657549	0077341751
3703547654	2700113851	1017857150	0089355151
3714037354	2692487851	1147475950	0100867651
3724246554	2685106951	1162580750	0102331251
3734493554	2677739351	1020547450	0089952451
3744778354	2670385151	7681882749	0067804751
3755027454	2663096451	4746281449	0041953951
3765193854	2655905851	3495239149	0030940951
3775475254	2648673251	2870938349	0025453151
3785872454	2641399151	2607434849	0023153351
3796384454	2634085251	2750003649	0024459151
3807012054	2626731951	3053003749	0027199851
3817754654	2619340751	3534026149	0031540251
3828565654	2611944351	3962053749	0035423751
3839489454	2604513051	4664394949	0041780351
3850548854	2597032451	5607456149	0050323851
3861744454	2589503351	6443931049	0057945251
3873076054	2581927151	7236733449	0065207351
3884543754	2574304951	7360099049	0066459151
3896147154	2566638251	8279905749	0074927751
3907625854	2559098751	8137323949	0073799551
3918999954	2551671451	8386989549	0076232851
3930538254	2544180851	9060481049	0082543651
3942240554	2536626651	8936147249	0081604151
3954106754	2529016251	8186760549	0074943951
3966136454	2521345551	7184487549	0065935151
3978330354	2513617351	6290232549	0057878851
3990688354	2505833451	5452301949	0050303851
4003210054	2497995451	4721214049	0043679551
4015895554	2490104651	3893818049	0036127751
4028745254	2482162451	3021963949	0028121251
4041758554	2474170651	2268871349	0021177351
4054936154	2466130151	1606527949	0015042051
4068277254	2458042951	1199576449	0011267851
4081782554	2449910151	8955797548	0008440251
4095451954	2441733051	6437633248	0006087751
4109284954	2433513451	3963700748	0003761451
4123281654	2425252751	1971993048	0001878151
4137442754	2416951951	9809442247	0000937751
4151767554	2408612751		
4166256354	2400236451		
4180908854	2391824551		
4195725454	2383378151		
4210706054	2374898751		
4225850454	2366387651		
4241158454	2357846451		

1200°K

$\bar{\nu}$	$\mu$	$E$	$\epsilon$
3000052754	3333274851		
3005790154	3326912351		
3011483454	3320622751		
3017133054	3314404851		
3022738454	3308258551	7706278348	0002802551
3028300054	3302182751	7690800848	0002790051
3033766554	3296232651	8771994148	0003174751
3039334554	3290194051	1094258549	0003950751
3044986654	3284086751	1316516249	0004741651
3050604654	3278038751	1532717149	0005507051
3056187654	3272050451	1529499749	0005482451
3061634454	3266229351	1417319149	0005068751
3067281054	3260216551	1196685149	0004269551
3073184754	3253953551	1085424549	0003863051
3079322354	3247467851	1299408749	0004612951
3085500054	3240965851	1404292549	0004972651
3091607754	3234563051	1508674149	0005328951
3097484854	3228425951	1612662049	0005682651
3103312954	3222362851	1724254649	0006061751
3109147654	3216315651	1827709549	0006410451
3115478654	3209779751	2144715849	0007503451
3121800054	3203280251	2460038149	0008585251
3127307154	3197639351	2454448949	0008547351
3133324554	3191498451	2448313149	0008506051
3139500054	3185220651	2441985949	0008463951
3145397254	3179248751	2435916249	0008423951
3151367154	3173226051	2441259049	0008423351
3157565854	3166996651	2434791149	0008381451
3164242354	3160314251	2533347849	0008698951
3172972054	3151619451	2734058449	0009357951
3179880054	3144772851	3249973049	0011095651
3186385054	3138352751	3571175549	0012163451
3192922854	3131926651	3141878749	0010676051
3199494054	3125494251	3863581849	0013097651
3206098354	3119056051	4684958349	0015845051
3212735954	3112611951	4048059949	0013659051
3219419754	3106149851	3535126049	0011900651
3226139054	3099680551	5493588849	0018450751
3232883554	3093213851	6199712249	0020774251
3239652654	3086750751	4864370349	0016262351
3246446454	3080291151	5467839549	0018238251
3253265554	3073834651	7095541449	0023613751
3260044554	3067442851	6457619749	0021442751
3266839154	3061062951	5749045749	0019047551
3273701154	3054646651	7571797649	0025030851
3280630154	3048194951	9177948749	0030273051
3287626454	3041708151	7250641949	0023862751
3294690054	3035186951	8446608449	0027737151
3301771854	3028676951	1039425250	0034057351
3308922954	3022131551	8732537849	0028549551
3316148354	3015546751	9861889849	0032170551
3323448154	3008923251	1316824450	0042861351
3330823054	3002261051	1054680850	0034253051
3338272254	2995561651	1192097150	0038630551
3345795954	2988825551	1590014650	0051411651
3353394354	2982053151	1303088950	0042041351
3361067354	2975245451	1344432650	0043279751
3368814854	2968403051	1778626150	0057131451
3376636954	2961526651	1492649250	0047840451

1200°K

$\bar{\nu}$	$\mu$	E	$\epsilon$
3384533754	2954616851	1742741250	0055733851
3392504954	2947674451	2092286950	0066766451
3400550854	2940700151	1579695250	0050299551
3408671454	2933694351	1739846050	0055278751
3416910254	2926620751	2429101050	0077009951
3425280954	2919468651	1771852650	0056050651
3433656554	2912347251	2252371950	0071097751
3442036954	2905256551	2729245750	0085967251
3450422254	2898196151	1920866450	0060377351
3458786754	2891187251	2814361350	0088278951
3467165554	2884200451	2407504150	0075362551
3475566754	2877228651	2251064850	0070322951
3483990154	2870272251	2951677350	0092025451
3492347854	2863403251	2269629550	0070622551
3500566254	2856680751	3043655350	0094527451
3508875754	2849915751	2872111650	0089030951
3517276254	2843109151	2229209650	0068971551
3525767854	2836261751	3144134150	0097096251
3534349954	2829374651	2322396950	0071585351
3543023654	2822448051	2800744750	0086168851
3551787754	2815483651	2611868450	0080208751
3560643154	2808481451	2517165450	0077157851
3569740754	2801323951	2704914950	0082758251
3579073554	2794019251	1799418150	0054950551
3588378854	2786773851	2327934750	0070959151
3597657054	2779586851	2001477450	0060897951
3606908454	2772457451	1973085950	0059927851
3616132254	2765385651	2032494550	0061625151
3625328954	2758370451	1719474350	0052045851
3634004654	2751785251	1729485050	0052266451
3642661854	2745245251	1641798350	0049539851
3651713954	2738440251	1895708250	0057110651
3661160654	2731374351	1847056550	0055554551
3671101954	2723977851	2034447450	0061088251
3682048754	2715879351	2281228350	0068374651
3692864054	2707925351	2487883350	0074438851
3703547654	2700113851	2828755250	0084495651
3714037354	2692487851	3025954950	0090240451
3724246554	2685106951	2962301150	0088206851
3734493554	2677739351	2409586050	0071641151
3744778354	2670385151	1567914450	0046548251
3755027454	2663096451	9958180449	0029521551
3765193854	2655905851	8618851849	0025515651
3775475254	2648673251	8233547349	0024341751
3785872454	2641399151	8132209349	0024009851
3796384454	2634085251	8352941549	0024628951
3807012054	2626731951	8792940649	0025892551
3817754654	2619340751	9560003149	0028115451
3828565654	2611944351	1037160550	0030464251
3839489454	2604513051	1242745850	0036458351
3850548854	2597032451	1334779350	0039111451
3861744454	2589503351	1454706550	0042575551
3873076054	2581927151	1699041850	0049669751
3884543754	2574304951	1921032450	0056096751
3896147154	2566638251	2077972050	0060613551
3907625854	2559098751	2269449150	0066130451
3918999954	2551671451	2223017250	0064713651
3930538254	2544180851	2468125350	0071780151
3942240554	2536628651	2603827350	0075656451
3954106754	2529016251	2513005350	0072951951
3966136454	2521345551	2414033350	0070018051

$\bar{\nu}$	$\mu$	E	$\epsilon$	1200°K
3978330354	2513617351	2307016150	0066858351	
3990688354	2505833451	2067989850	0059883351	
4003210054	2497995451	1756030450	0050811051	
4015895554	2490104651	1616640550	0046743851	
4028745254	2482162451	1309732550	0037843951	
4041758554	2474170651	1158887150	0033463751	
4054936154	2466130151	8556545449	0024692851	
4068277254	2458042951	7315774649	0021100451	
4081782554	2449910151	5363623949	0015462051	
4095451954	2441733051	4064956049	0011712851	
4109284954	2433513451	2935803749	0008455751	
4123281654	2425252751	2448293249	0007049051	
4137442754	2416951951	1650568849	0004750851	
4151767554	2408612751	1016731549	0002925751	
4166256354	2400236451	1011556649	0002910251	
4180908854	2391824551	8514485448	0002449251	
4195725454	2383378151	6158982548	0001771551	
4210706054	2374898751	3828038948	0001101051	
4225850454	2366387651	3044999148	0000875851	
4241158454	2357846451	2270401048	0000653151	
4256630854	2349275951	1514968348	0000435951	
4272267154	2340677651	1505717548	0000433351	
4288067354	2332053051	1496289648	0000430751	
4304030854	2323403451	1497306448	0000431251	
4320158954	2314729751	7437689247	0000214351	
4336450854	2306033351	7387997147	0000212951	
4352906654	2297315551			
4369526354	2288577651			
4386309754	2279820851			
4403257354	2271046051			
4420368854	2262254751			
4437643954	2253448151			
4453654554	2245347151			
4468980554	2237646851			

$\bar{\nu}$	$\mu$	$E$	$\epsilon$	1500°K
2899688054	3448646951	2043626949	0004034551	
2903741054	3443833351	2232777249	0004395451	
2907961954	3438834651	2425084949	0004759951	
2912347954	3433655751	2594920249	0005077751	
2916900054	3428297251	2750657149	0005365551	
2921618354	3422760651	2904237849	0005646651	
2926502454	3417048351	3055662649	0005921151	
2931647554	3411051351	3189496149	0006158651	
2936787554	3405081251	3154218649	0006069151	
2941808454	3399269651	2955486649	0005667351	
2946974454	3393310851	3114579849	0005951551	
2952505854	3386953551	3272710449	0006230351	
2957800054	3380891251	3430477249	0006507551	
2962557854	3375437851	3751346649	0007093451	
2967500054	3369839951	3908127049	0007365651	
2972514854	3364154851	3883411049	0007294651	
2977762054	3358226751	4199661049	0007861351	
2983368654	3351915751	4191733749	0007817551	
2988949554	3345657151	4022870449	0007475151	
2994463154	3339496851	3533434849	0006542051	
3000052754	3333274851	3206003649	0005914251	
3005790154	3326912351	3679523649	0006762551	
3011483454	3320622751	4470441149	0008185951	
3017133054	3314404851	4461473449	0008139851	
3022738454	3308258551	3975461249	0007227151	
3028300054	3302182751	4443573749	0008049551	
3033766554	3296232651	4909879749	0008863451	
3039334554	3290194051	5215965449	0009382951	
3044986654	3284086751	5546433949	0009941951	
3050604654	3278038751	5218536949	0009321351	
3056187654	3272050451	4576360149	0008145851	
3061634454	3266229351	4094477549	0007263451	
3067281054	3260216551	4557073749	0008055951	
3073184754	3253953551	5330640349	0009389151	
3079322354	3247467851	6100001849	0010703951	
3085500054	3240965851	6397332749	0011183451	
3091607754	3234563051	6693244049	0011657451	
3097484854	3228425951	6367028749	0011049951	
3103312954	3222362851	6226475349	0010768151	
3109147654	3216315651	6988301349	0012043451	
3115478654	3209779751	8364391349	0014360651	
3121800054	3203280251	9115213749	0015591151	
3127307154	3197639351	8632071549	0014716851	
3133324554	3191498451	8456733049	0014366951	
3139500054	3185220651	9815131149	0016614551	
3145397254	3179248751	1024967650	0017290651	
3151367154	3173226051	9505578449	0015980051	
3157565854	3166996651	9327485049	0015624651	
3164242354	3160314251	1006302050	0016792251	
3172972054	3151619451	1139191050	0018915351	
3179880054	3144772851	1256689250	0020788051	
3186385054	3138352751	1304762950	0021500851	
3192922854	3131926651	1270715450	0020863051	
3199494054	3125494251	1357474750	0022205851	
3206098354	3119056051	1548928250	0025244951	
3212735954	3112611951	1454303050	0023615951	
3219419754	3106149851	1336647350	0021625851	
3226139054	3099680551	1901449750	0030651051	
3232883554	3093213851	2044756950	0032840551	



$\bar{\nu}$	$\mu$	E	$\epsilon$
3239652654	3086750751	1659405850	0026554051
3246446454	3080291151	1862733750	0029699051
3253265554	3073834651	2168653350	0034450651
3260044554	3067442851	2072816250	0032809751
3266839154	3061062951	1987071150	0031339651
3273701154	3054640651	2586462450	0040646051
3280630154	3048194951	2666137450	0041746451
3287626454	3041708151	2227368250	0034749851
3294690054	3035186951	2748832350	0042728451
3301771854	3028676951	3076381550	0047646051
3308922954	3022131551	2640069650	0040739351
3316148354	3015546751	3025216650	0046511351
3323448154	3008923251	3760265150	0057599551
3330823054	3002261051	3017559050	0046051851
3338272254	2995561651	3297910950	0050143451
3345795954	2988825551	4244511650	0064295551
3353394354	2982053151	3445946250	0052003651
3361067354	2975245451	3492626450	0052510251
3368814854	2968403051	4517621650	0067664751
3376636954	2961526651	4024624350	0060052951
3384533754	2954616851	4243436350	0063077951
3392504954	2947674451	5156347250	0076356851
3400550854	2940700151	4135729950	0061009851
3408671454	2933694351	4373102150	0064265051
3416910254	2926620751	5611081150	0082140451
3425280954	2919466651	4355124650	0063506951
3433656554	2912347251	5403516350	0078490651
3442036954	2905256551	5814805550	0084141151
3450422254	2898196151	4591444650	0066185851
3458786754	2891187251	6097782650	0087568051
3467165554	2884200451	5580836750	0079843651
3475566754	2877228651	4898240150	0069816051
3483990154	2870272251	6305030550	0089533251
3492347854	2863403251	5223140050	0073898351
3500566254	2856680751	5903329850	0083223051
3508875754	2849915751	6222908750	0087413251
3517276254	2843109151	4857474950	0067987051
3525767854	2836261751	6192991850	0086365951
3534349954	2829374651	5298856050	0073628351
3543023654	2822448051	5516618450	0076375151
3551787754	2815483651	5663857950	0078155051
3560643154	2808481451	5106608850	0070182951
3569740754	2801323951	5502956850	0075348051
3579073554	2794019251	4216721450	0057517351
3588378854	2786773851	4557536050	0061932851
3597657054	2779586851	4580944750	0062019851
3606908454	2772457451	4197802450	0056624051
3616132254	2765385651	4389623350	0058996551
3625328954	2758370451	3923093650	0052537151
3634004654	2751785251	4135347550	0055193551
3642661854	2745245251	3966593950	0052765051
3651713954	2738440251	4304973350	0057068751
3661160654	2731374351	4541226650	0059985751
3671101954	2723977851	4664744150	0061387851
3682048754	2715879351	5294702650	0069395151
3692864054	2707925351	5583915550	0072894951
3703547654	2700113851	5977125350	0077724951
3714037354	2692487851	6052970150	0078413851
3724246554	2685106951	5602962750	0072319951
3734493554	2677739351	4322112550	0055585451
3744778354	2670385151	2834609350	0036323951

$\bar{\nu}$	$\mu$	E	$\epsilon$	1500°K
3755027454	2663096451	1993827150	0025459051	
3765193854	2655905851	1827685650	0023256151	
3775475254	2648673251	1887351850	0023931451	
3785872454	2641399151	2026598350	0025607251	
3796384454	2634085251	2045865350	0025760151	
3807012054	2626731951	2075848350	0026046051	
3817754654	2619340751	2319894250	0029006151	
3828565654	2611944351	2478708850	0030883651	
3839489454	2604513051	2828606450	0035120151	
3850548854	2597032451	3054952450	0037797951	
3861744454	2589503351	3286559150	0040521251	
3873076054	2581927151	3694451650	0045390751	
3884543754	2574304951	4123697850	0050487051	
3896147154	2566638251	4535328850	0055332151	
3907625854	2559098751	4877802550	0059306551	
3918999954	2551671451	4933413750	0059781451	
3930538254	2544180851	5529496150	0066779251	
3942240554	2536628651	5744421150	0069141051	
3954106754	2529016251	5655885150	0067845651	
3966136454	2521345551	5651242650	0067560851	
3978330354	2513617351	5525958150	0065839651	
3990688354	2505833451	5054167250	0060014651	
4003210054	2497995451	4465648650	0052847151	
4015895554	2490104651	4174960750	0049240051	
4028745254	2482162451	3525159850	0041435851	
4041758554	2474170651	3113777550	0036477051	
4054936154	2466130151	2518530350	0029404651	
4068277254	2458042951	2136670850	0024862551	
4081782554	2449910151	1815448950	0021054151	
4095451954	2441733051	1393066650	0016101851	
4109284954	2433513451	1100265250	0012675251	
4123281654	2425252751	8669941349	0009954951	
4137442754	2416951951	6811871349	0007795751	
4151767554	2408612751	5535538449	0006314351	
4166256354	2400236451	4383412049	0004983851	
4180908854	2391824551	3465997649	0003928051	
4195725454	2383378151	3113707649	0003517451	
4210706054	2374898751	2764694649	0003113251	
4225850454	2366387651	2529041049	0002838851	
4241158454	2357846451	2404943249	0002691151	
4256630854	2349275951	2188287549	0002441051	
4272267154	2340677651	1957432749	0002176851	
4288067354	2332053051	1729045849	0001917051	
4304030854	2323403451	1513943249	0001673451	
4320158954	2314729751	1396632749	0001539251	
4336450854	2306033351	1280586149	0001407151	
4352906654	2297315551	1059856849	0001161251	
4369526354	2288577651	1052440349	0001149851	
4386309754	2279820851	1052705649	0001146851	
4403257354	2271046051	9405540048	0001021851	
4420368854	2262254751	9335728648	0001011551	
4437643954	2253448151	9194746348	0000993551	
4453654554	2245347151	9065371348	0000977151	
4468980554	2237646851	8942693248	0000961751	
4484599754	2229853451	8818842948	0000946351	

$\bar{v}$	$\mu$	$E$	$\epsilon$
3000052754	3333274851	8318279249	0008762351
3005790154	3326912351	1011760850	0010609151
3011483454	3320622751	1087404650	0011350851
3017133054	3314404851	1085223250	0011277551
3022738454	3308258551	1031471050	0010671651
3028300054	3302182751	1158074250	0011929251
3033766554	3296232651	1309872050	0013435251
3039334554	3290194051	1537876750	0015705451
3044986654	3284086751	1439074750	0014631951
3050604654	3278038751	1282195750	0012980151
3056187654	3272050451	1279504250	0012897151
3061634454	3266229351	1276864050	0012816651
3067281054	3260216551	1477969950	0014771151
3073184754	3253953551	1703431950	0016947651
3079322354	3247467851	1826196050	0018084251
3085500054	3240965851	1897692650	0018704351
3091607754	3234563051	1994090350	0019563851
3097484854	3228425951	1913886050	0018693951
3103312954	3222362851	1842700050	0017920051
3109147654	3216315651	1964279350	0019019151
3115478654	3209779751	2536947450	0024448251
3121800054	3203280251	2555433250	0024511051
3127307154	3197639351	2449641950	0023400651
3133324554	3191498451	2642988950	0025135851
3139500054	3185220651	2810244550	0026605451
3145397254	3179248751	2753644450	0025957251
3151367154	3173226051	2660236050	0024967751
3157565854	3166996651	2901149350	0027106451
3164242354	3160314251	2966983950	0027587851
3172972054	3151619451	3374468350	0031179951
3179880054	3144772851	3560708650	0032738151
3186385054	3138352751	3838020150	0035124251
3192922854	3131926651	3434365950	0031284251
3199494054	3125494251	3864522550	0035039051
3206098354	3119056051	4194421150	0037853251
3212735954	3112611951	3598275350	0032322051
3219419754	3106149851	3847985450	0034403651
3226139054	3099680551	5244262050	0046668151
3232883554	3093213851	4913225050	0043517951
3239652654	3086750751	4145483950	0036546251
3246446454	3080291151	5147186350	0045165351
3253265554	3073834651	5491887350	0047965051
3260044554	3067442851	4705852850	0040910051
3266839154	3061062951	5410540050	0046819251
3273701154	3054646651	6902558850	0059453051
3280630154	3048194951	5756659050	0049351951
3287626454	3041708151	5740896450	0048985951
3294690054	3035186951	7222687050	0061339251
3301771854	3028676951	6564113850	0055483851
3308922954	3022131551	5850964850	0049221851
3316148354	3015546751	8096879850	0067791651
3323448154	3008923251	7639954050	0063659751
3330823054	3002261051	6223566750	0051607951
3338272254	2995561651	8542542850	0070494751
3345795954	2988825551	8745170850	0071815551
3353394354	2982053151	6949807650	0056792651
3361067354	2975243451	8554329850	0069560651
3368814854	2968403051	9385543150	0075942551
3376636954	2961526651	7831701450	0063054951
3384533754	2954616851	9493789450	0076055351
3392504954	2947674451	1017333351	0081090651

$\bar{\nu}$	$\mu$	E	$\epsilon$
3400550854	2940700151	7770392750	0061625251
3408671454	2933694351	9900494050	0078121551
3416910254	2926620751	1052725651	0082643051
3425280954	2919468651	8254711350	0064468351
3433656554	2912347251	1130861851	0087865351
3442036954	2905256551	1045683951	0080831751
3450422254	2898196151	8724582250	0067098051
3458786754	2891187251	1182049251	0090448551
3467165554	2884200451	9482640450	0072189851
3475566754	2877228651	9300684950	0070455051
3483990154	2870272251	1126032451	0084870751
3492347854	2863403251	8785327250	0065888951
3500566254	2856680751	1132165951	0084500351
3508875754	2849915751	1015847851	0075449851
3517276254	2843109151	9104279250	0067289151
3525767854	2836261751	1080147051	0079440051
3534349954	2829374651	8992402650	0065807951
3543023654	2822448051	1062459851	0077365951
3551787754	2815483651	9187877950	0066569651
3560643154	2808481451	9208457750	0066383651
3569740754	2801323951	9169115750	0065760851
3579073554	2794019251	7465670750	0053263551
3588378854	2786773851	8494681650	0060290551
3597657054	2779586851	7836223450	0055331151
3606908454	2772457451	7968349450	0055977151
3616132254	2765385651	7736296250	0054072251
3625328954	2758370451	7322904150	0050926451
3634004654	2751785251	8010542450	0055446551
3642661854	2745245251	7668417550	0052830851
3651713954	2738440251	8583242650	0058846551
3661160654	2731374351	8721915650	0059496251
3671101954	2723977851	8605429050	0058392551
3682048754	2715879351	9453738750	0063779451
3692864054	2707925351	9615332250	0064503151
3703547654	2700113851	1000602451	0066751951
3714037354	2692487851	9614395850	0063792451
3724246554	2685106951	8611249450	0056837751
3734493554	2677739351	6476807850	0042526651
3744778354	2670385151	4336028350	0028322251
3755027454	2663096451	3417989350	0022210851
3765193854	2655905851	3393352850	0021938851
3775475254	2648673251	3689454650	0023731651
3785872454	2641399151	3977142350	0025451051
3796384454	2634085251	3913089650	0024912351
3807012054	2626731951	4207800850	0026650251
3817754654	2619340751	4612916950	0029064551
3828565654	2611944351	4770428450	0029901251
3839489454	2604513051	5469031050	0034101751
3850548854	2597032451	5812666550	0036055051
3861744454	2589503351	6225095250	0038410351
3873076054	2581927151	7125013950	0043730951
3884543754	2574304951	7520357950	0045912651
3896147154	2566638251	8491010150	0051562451
3907625854	2559098751	8845535550	0053434451
3918999954	2551671451	9037553350	0054313551
3930538254	2544180851	9910618850	0059251951
3942240554	2536628651	1017816651	0060534251
3954106754	2529016251	1012994351	0059931351
3966136454	2521345551	1021708351	0060127951
3978330354	2513617351	9874608550	0057804151
3990688354	2505833451	9358492550	0054490651

$\bar{\nu}$  $\mu$  $E$  $\epsilon$ 

1800°K

4003210054	2497995451	8516112550	0049320051
4015895554	2490104651	7917699050	0045607451
4028745254	2482162451	7088429350	0040609851
4041758554	2474170651	6302220150	0035909551
4054936154	2466130151	5426562850	0030751551
4068277254	2458042951	4707705850	0026531951
4081782554	2449910151	3881541450	0021755751
4095451954	2441733051	3173839450	0017691251
4109284954	2433513451	2546221850	0014114551
4123281654	2425252751	2053407150	0011319751
4137442754	2416951951	1638531350	0008982651
4151767554	2408612751	1282364150	0006991051
4166256354	2400236451	9113122249	0004940551
4180908854	2391824551	8158843249	0004398551
4195725454	2383378151	7573883349	0004060451
4210706054	2374898751	5917940849	0003155051
4225850454	2366387651	5527633349	0002930451
4241158454	2357846451	5318056449	0002803651
4256630854	2349275951	4790575549	0002511451
4272287154	2340677651	4232286849	0002206451
4288067354	2332053051	3154339849	0001635351
4304030854	2323403451	2981123649	0001536851
4320158954	2314729751	2787457949	0001429051
4336450854	2306033351	2249678449	0001146951
4352906654	2297315551	1890555349	0000958551
4369526354	2288577651	1706659949	0000860551
4386309754	2279820851	1536381149	0000770351
4403257354	2271046051	1864161149	0000929551
4420368854	2262254751	1682113349	0000834251
4437643954	2253448151		
4453654554	2245347151		
4468980554	2237646851		

$\bar{\nu}$	$\mu$	E	$\epsilon$
3004073554	3328813451	2147939550	0014390851
3009780254	3322501851	2411590250	0016074251
2998344254	3335174151	1883201750	0012682751
3015442654	3316262851	2395813850	0015887951
3021061554	3310094851	2353052650	0015525951
3026636054	3303998251	2575585250	0016909751
3032117654	3298025151	2897493950	0018930451
3037642954	3292026251	2966739450	0019287851
3043294854	3285912451	3072976950	0019878651
3048922854	3279846951	2916954350	0018775651
3054516254	3273840951	2798879350	0017927051
3059990454	3267984151	2730963150	0017408051
3065557054	3262049951	2911828450	0018470651
3071395854	3255848751	3330163150	0021016751
3077451654	3249441851	3732989550	0023434951
3083656054	3242903951	3723955750	0023252651
3089792654	3236463251	3881289250	0024106651
3095751554	3230233451	3946586250	0024386451
3101556354	3224187851	3863144550	0023751951
3107367654	3218158051	3742935350	0022898451
3113477754	3211842551	4177268450	0025422451
3119959954	3205169451	4889144650	0029590951
3125613854	3199371651	4729954350	0028490251
3131434054	3193425151	4902860150	0029386451
3137667754	3187080651	5073936650	0030252151
3143612954	3181053251	5281304350	0031331351
3149572954	3175033751	5108599150	0030155551
3155715754	3168853351	5278495450	0030998751
3162045054	3162510351	5556594950	0032460151
3170331154	3154244751	5609508050	0032544351
3177935154	3146697451	6099131150	0035163051
3184430154	3140279351	6619133050	0037957251
3190957954	3133855251	6599964950	0037644851
3197519254	3127424551	6399828750	0036307751
3204113654	3120988051	7137888250	0040277551
3210741154	3114545751	6972684450	0039133751
3217408854	3108091251	6521484150	0036404151
3224120754	3101620951	7573025850	0042045451
3230857754	3095153351	8653347150	0047783551
3237619054	3088689651	7988782350	0043875251
3244405654	3082228751	7536745150	0041168651
3251217354	3075771051	8965394150	0048707351
3258019254	3069349651	8618509550	0046570651
3264793654	3062980851	7886427450	0042387051
3271635454	3056575351	9369363450	0050086351
3278544354	3050134251	1042216651	0055412851
3285520554	3043657851	8999701850	0047589251
3292563754	3037147051	9910789650	0052119751
3299641354	3030632551	1123234251	0058745651
3306769754	3024099351	9979690250	0051906851
3313973154	3017526051	1035801351	0053575951
3321250554	3010914151	1228082351	0063167151
3328602654	3004263751	1045288951	0053463151
3336029654	2997575351	1065224651	0054174951
3343531154	2990850051	1295066851	0065489651
3351107054	2984088551	1160653451	0058356851
3358757554	2977291551	1145861251	0057281551
3366482754	2970459351	1326430451	0065924451
3374282654	2963592951	1235613651	0061053351
3382156854	2956693251	1270304151	0062400051
3390105854	2949760451	1420522051	0069368551

2200°K

$\bar{\nu}$	$\mu$	$E$	$\epsilon$
3398129054	2942795951	1265513351	0061433451
3406227354	2935799451	1310064751	0063218051
3414400054	2928772351	1517144251	0072773251
3422769254	2921611051	1293987851	0061690851
3431143454	2914480351	1392538851	0065986251
3439522254	2907380651	1510899751	0071161751
3447906154	2900311051	1291971951	0060483751
3456277554	2893286251	1494057451	0069525251
3464649454	2886294951	1443978151	0066793751
3473043854	2879318751	1316771351	0060546651
3481460754	2872357651	1473403451	0067345751
3489900054	2865411651	1320533651	0059999951
3498091254	2858701951	1390413751	0062812351
3506373354	2851949651	1472662451	0066143351
3514746754	2845155251	1301522251	0058116551
3523210554	2838320351	1501145751	0066637651
3531765854	2831444851	1314585751	0058012051
3540411854	2824530251	1360895151	0059699351
3549149154	2817576851	1331123351	0058044851
3557977254	2810585751	1263935851	0054784151
3566935554	2803527051	1294706651	0055777651
3576276354	2796204551	1112217551	0047614151
3585590154	2788941251	1129900251	0048069051
3594876654	2781736751	1119450051	0047329251
3604135654	2774590451	1139835051	0047894651
3613367754	2767501451	1150862851	0048062851
3622572954	2760468951	1077831251	0044740051
3631484654	2753694751	1147075951	0047336351
3640023254	2747235251	1175537351	0048240551
3648956954	2740509251	1227963051	0050099451
3658284954	2733521451	1230531351	0049901451
3668007954	2726275551	1184530951	0047735551
3678778554	2718293651	1204875751	0048220851
3689633154	2710296651	1219585451	0048472351
3700356354	2702442551	1255794851	0049572751
3710947954	2694729351	1240765051	0048652851
3721179954	2687319751	1121116251	0043679451
3731415454	2679948251	9205807250	0035637651
3741688954	2672589951	6411891750	0024663751
3752000054	2665245251	5333328450	0020384551
3762131754	2658067551	5127398750	0019475551
3772378854	2650847351	5686644750	0021464651
3782741154	2643585651	6078352750	0022798851
3793218854	2636283551	6102720950	0022745351
3803811454	2628942151	6382546350	0023636851
3814519954	2621561951	6853754050	0025219451
3825315054	2614163851	7163099650	0026188651
3836197754	2606747851	7818710050	0028401651
3847216854	2599281651	8550838650	0030859951
3858371454	2591767151	9086680350	0032579951
3869662454	2584204851	9584375050	0034138851
3881089154	2576596351	1061702851	0037567351
3892652054	2568942751	1110113251	0039019251
3904245454	2561314451	1171637851	0040909051
3915570554	2553906351	1245841051	0043220151
3927059654	2546434551	1323602251	0045619851
3938712454	2538900851	1396121651	0047804551
3950529554	2531306251	1387343051	0047190651
3962510454	2523652751	1389254151	0046941651
3974655054	2515941651	1368648851	0045935751
3986963754	2508174351	1346068151	0044873251

2200°K

$\bar{\nu}$	$\mu$	E	$\epsilon$
3999436154	2500352551	1256622951	0041606951
4012072754	2492477351	1187322651	0039043651
4024873054	2484550451	1081918151	0035332851
4037837454	2476573251	9906971550	0032129751
4050965554	2468547351	8622625550	0027769751
4064257654	2460474051	7732879650	0024729851
4077713854	2452354651	6767355450	0021489751
4091334054	2444190651	5727500150	0018058951
4105117554	2435983951	4750552450	0014872051
4119065654	2427735151	4025204650	0012511251
4133177254	2419446251	3327190950	0010267351
4147453054	2411118351	2771997250	0008492451
4161892354	2402753251	2329122650	0007083951
4176495754	2394351851	1810645750	0005467051
4191263254	2385915551	1641727250	0004920851
4206194754	2377445851	1421741950	0004230251
4221289754	2368944351	1204024650	0003556151
4236549054	2360411751	1126195950	0003301851
4251972054	2351849951	1126864450	0003279351
4267559154	2343259951	1041712150	0003009151
4283309754	2334643251	9574261349	0002745151
4299224754	2326000851	7712075149	0002194751
4315303554	2317334151	7456780249	0002106351
4331546254	2308644451	6944076349	0001946851
4347952554	2299933151	6431078149	0001789551
4364523154	2291201151	6130376249	0001693051
4381257454	2282449851	6130991949	0001680551
4398155954	2273680251	6387091149	0001737651
4415217854	2264893951	6339741049	0001711851